JPET Fast Forward. Published on May 25, 2016 as DOI: 10.1124/jpet.116.233312
This article has not been copyedited and formatted. The final version may differ from this version.

Differential regulation of gene expression by cholesterol biosynthesis inhibitors that reduce (pravastatin) or enhance (squalestatin 1) nonsterol isoprenoid levels in primary cultured mouse and rat hepatocytes.

Elizabeth A. Rondini, Zofia Duniec-Dmuchowski, Daniela Cukovic, Alan A. Dombkowski, and Thomas A. Kocarek

Institute of Environmental Health Sciences, Wayne State University, Detroit, MI 48202, USA (E.A.R., Z.D-D, T.A.K.)

Department of Pediatrics, Division of Clinical Pharmacology and Toxicology, Wayne State University, Detroit, MI 48202 (D.C., A.A.D)

JPET Fast Forward. Published on May 25, 2016 as DOI: 10.1124/jpet.116.233312
This article has not been copyedited and formatted. The final version may differ from this version.

Running title: Regulation of hepatocellular gene expression by isoprenoids

Address correspondence to: Dr. Thomas A. Kocarek, Institute of Environmental Health Sciences, 6135 Woodward Avenue, IBio Building, Room 2126, Wayne State University, Detroit, MI 48202, USA. Tel: (313) 577-6580; FAX: (313) 972-8025; E-mail: t.kocarek@wayne.edu

Number of text pages: 43

Number of tables: 2 Supplemental

Number of figures: 8

Number of references: 77

Number of words in Abstract: 249

Number of words in Introduction: 745

Number of words in Discussion: 1500

Abbreviations: ACOT, acetyl-coenzyme A thioesterase; CVD, cardiovascular disease; CoA, Coenzyme A; CAR, constitutive androstane receptor (*NR1I3*); Cipro, ciprofibrate; C_T, cycle threshold; CYP, cytochrome P450; DCA, dicarboxylic acid; DMSO, dimethyl sulfoxide; FPP, farnesyl pyrophosphate; FXR, farnesoid X receptor (*NR1H4*); GGOH, geranylgeraniol; GGPP, geranylgeranyl pyrophosphate; HDL, high-density lipoprotein; HMGCR, 3-hydroxy-3-methylglutaryl-CoA reductase; LDL, low-density lipoprotein; MVA, mevalonate; PPARα, peroxisome proliferator-activated receptor α (*NR1C1*); PPARγ, peroxisome proliferator-activated receptor γ (*NR1C3*); PB, phenobarbital; Prav, pravastatin; PCR, polymerase chain reaction; *q*RT-PCR, quantitative reverse transcription-polymerase chain reaction; SREBP, sterol regulatory

JPET Fast Forward. Published on May 25, 2016 as DOI: 10.1124/jpet.116.233312
This article has not been copyedited and formatted. The final version may differ from this version.

element-binding protein; SSI, squalene synthase inhibitor; SQ1, squalestatin 1 (zaragozic acid A); TBP, TATA box binding protein; TCPOBOP, 1,4-bis-[2-(3,5-dichloropyridyloxy)]benzene.

JPET Fast Forward. Published on May 25, 2016 as DOI: 10.1124/jpet.116.233312
This article has not been copyedited and formatted. The final version may differ from this version.

Abstract.

Squalene synthase inhibitors (SSIs), such as squalestatin 1 (SQ1), reduce cholesterol biosynthesis but cause accumulation of farnesyl pyrophosphate (FPP)-derived isoprenoids that can modulate the activity of nuclear receptors, including the constitutive androstane receptor (CAR), farnesoid X receptor, and peroxisome proliferator-activated receptors (PPARs). In comparison, 3-hydroxy-3-methylglutaryl-coenzyme A reductase inhibitors (e.g., pravastatin) inhibit production of both cholesterol and nonsterol isoprenoids. To characterize the effects of isoprenoids on hepatocellular physiology, microarrays were used to compare orthologous gene expression from primary cultured mouse and rat hepatocytes that were treated with either SQ1 or pravastatin. Compared to controls, 47 orthologs were affected by both inhibitors, 90 were affected only by SQ1, and 51 were unique to pravastatin treatment ($P<0.05$, $\geq$1.5-fold change). When the effects of SQ1 and pravastatin were compared directly, 162 orthologs were found to be differentially co-regulated between the two treatments. Genes involved in cholesterol and unsaturated fatty acid biosynthesis were upregulated by both inhibitors, consistent with cholesterol depletion; however, the extent of induction was greater in rat than in mouse hepatocytes. SQ1 induced several orthologs associated with microsomal, peroxisomal, and mitochondrial fatty acid oxidation and repressed orthologs involved in cell cycle regulation. In comparison, pravastatin repressed the expression of orthologs involved in retinol and xenobiotic metabolism. Several of the metabolic genes altered by isoprenoids were inducible by a PPARα agonist, whereas CYP2B was inducible by activators of CAR. Our findings indicate that SSIs uniquely influence cellular lipid metabolism and cell cycle regulation, probably due to FPP catabolism through the farnesol pathway.

JPET Fast Forward. Published on May 25, 2016 as DOI: 10.1124/jpet.116.233312
This article has not been copyedited and formatted. The final version may differ from this version.

Introduction.

Cardiovascular disease (CVD) is the leading cause of mortality worldwide, and elevated low-density lipoprotein (LDL)-cholesterol is a major risk factor for CVD development (Mathers et al., 2009; Goldstein and Brown, 2015). Inhibitors of 3-hydroxy-3-methylglutaryl-coenzyme A reductase (HMGCR, *ie*, statins), the rate limiting enzyme in cholesterol biosynthesis (**Fig. 1**), are the most widely used class of anti-cholesterol drugs. Various clinical trials have demonstrated the efficacy of statin therapy in lowering LDL-cholesterol and reducing both CVD morbidity and mortality (Cholesterol Treatment Trialists et al., 2010; Cholesterol Treatment Trialists et al., 2015). However, statin use in some individuals is limited due to the development of adverse reactions, such as myopathies (Tomaszewski et al., 2011). Additionally, despite aggressive statin therapy, certain populations have high residual risk for CVD (Campbell et al., 2007; Sampson et al., 2012), therefore alternative lipid-modifying agents are needed.

Squalene synthase inhibitors [SSIs; e.g., squalestatin 1 (SQ1)] are a class of anti-cholesterol drugs that block the first committed step in sterol synthesis, in which farnesyl pyrophosphate (FPP) is converted to squalene (**Fig. 1**) (Do et al., 2009). Compared to inhibitors of HMGCR, SSIs preserve the synthesis of nonsterol isoprenoids that are utilized in the post-translational modification of proteins, glycoprotein synthesis, and for components of aerobic metabolism (Krag, 1998; Edwards and Ericsson, 1999; Dallner and Sindelar, 2000; McTaggart, 2006). Additionally, FPP can be dephosphorylated to farnesol, and then further metabolized to produce farnesoic acid and a number of chain-shortened dicarboxylic acids (DCAs) that are detectable in the urine (Bostedor et al., 1997; Vaidya et al., 1998). Several of these isoprenoid compounds function as signaling molecules that can modulate the activities of nuclear receptors

JPET Fast Forward. Published on May 25, 2016 as DOI: 10.1124/jpet.116.233312
This article has not been copyedited and formatted. The final version may differ from this version.

including peroxisome proliferator-activated receptors-α and γ (PPARα; PPARγ), the constitutive androstane receptor (CAR), and farnesoid X receptor (FXR) (Forman et al., 1995; Kocarek and Mercer-Haines, 2002; Takahashi et al., 2002; Rondini et al., 2016). Therefore, compared to statins, SSIs likely have distinctive effects on hepatic metabolism.

Similar to statins, treatment with SSIs has been shown to lower non-high-density lipoprotein (HDL) cholesterol in preclinical models (Hiyoshi et al., 2000; Hiyoshi et al., 2001; Nishimoto et al., 2003). SSIs also markedly reduced serum triglycerides through an LDL receptor-independent mechanism (Hiyoshi et al., 2001). The effect on triglyceride levels is thought to be mediated through farnesol and/or a farnesol metabolite (Hiyoshi et al., 2003), as farnesol treatment also decreased triglyceride biosynthesis and reduced hepatic steatosis, in part through PPARα activation (Duncan and Archer, 2008; Goto et al., 2011a). Elevated triglycerides are a known risk factor for CVD and commonly associated with metabolic dyslipidemia (Eckel et al., 2005; Boullart et al., 2012). Although the SSI lapaquistat (TAK-475) showed promising effects on serum lipid profiles in primates (Nishimoto et al., 2003), it's development was terminated during phase III clinical trials due to safety concerns and lack of commercial viability at lower doses (Stein et al., 2011). Nonetheless, there is still significant interest in SSI and the isoprenoid pathway with respect to hepatic lipid metabolism (Goto et al., 2011a; Nagashima et al., 2015) and as a potential therapeutic target for a variety of other conditions (Shang et al., 2014; Yang et al., 2014; Saito et al., 2015; Healey et al., 2016).

The liver is central to cholesterol metabolism and is a major target for hypolipidemic drugs. Previous studies have compared the effect of different statins on hepatocellular gene expression (Hafner et al., 2011; Leszczynska et al., 2011; Schroder et al., 2011). However, a detailed evaluation of SSI treatment on global gene responses has not been previously

JPET Fast Forward. Published on May 25, 2016 as DOI: 10.1124/jpet.116.233312
This article has not been copyedited and formatted. The final version may differ from this version.

performed, which is important for understanding both the beneficial as well as potentially adverse effects of isoprenoids on hepatocellular physiology. In the current investigation we therefore evaluated the effects of SQ1 on orthologous gene expression changes in primary cultured rodent hepatocytes using microarrays. Both mouse and rat hepatocytes were included to focus our analysis on conserved responses that are likely indicative of isoprenoid signaling mechanisms across species. Additionally, because SSIs also reduce cholesterol biosynthesis, effects of SQ1 were compared to those of the HMGCR inhibitor, pravastatin (Prav). Prav was selected because unlike other statins, it is not extensively metabolized (Hatanaka, 2000) and it does not produce off-target effects such as activation of xenobiotic-sensing receptor(s) (Kocarek and Reddy, 1996; Kocarek et al., 2002). Therefore, Prav was used to distinguish gene expression changes that were due to hepatic sterol depletion (Prav and SQ1) from those due to endogenous isoprenoid accumulation (SQ1). Treatment-induced changes were further validated using more sensitive methods and informative signaling pathways are discussed.

Material and Methods.

Materials. SQ1 was generously supplied from GlaxoSmithKline (Research Triangle Park, NC) and Prav from Bristol-Myers Squibb (Wallingford, CT). Cell culture medium and reagents were purchased from Invitrogen (Carlsbad, CA), primers from Integrated DNA Technologies (IDT; Coralville, IA), PureCol from Advanced Biomatrix (San Diego, CA), phenobarbital (PB), dimethyl sulfoxide (DMSO), 1,4-bis-[2-(3,5-dichloropyridyloxy)]benzene **(**TCPOBOP), and ciprofibrate (Cipro) from Sigma-Aldrich (St. Louis, MO), Matrigel from Corning (Tewksbury,

JPET Fast Forward. Published on May 25, 2016 as DOI: 10.1124/jpet.116.233312
This article has not been copyedited and formatted. The final version may differ from this version.

MA), and the cDNA synthesis kit and SYBR green master mix from Life Technologies (Carlsbad, CA). Other sources of reagents are provided below.

Primary Culture of Mouse and Rat Hepatocytes. Animal procedures were conducted in accordance with the regulatory guidelines of the Division of Laboratory Animal Resources at Wayne State University (Detroit, MI). Adult male and female C57BL/6 mouse breeder pairs were generously donated by Dr. Masahiko Negishi (National Institute of Environmental Health Sciences; Research Triangle Park, North Carolina) and used for colony generation. Male offspring (7-8 weeks of age) produced from this colony were then used for primary hepatocyte isolation. Adult male Sprague-Dawley rats (175–200 g) were purchased from Harlan Sprague Dawley (Indianapolis, IN) and, upon receipt, allowed one week to acclimatize prior to use. All animals were housed in an Association for Assessment and Accreditation of Laboratory Animal Care-approved animal facility in temperature (23±2 ºC) and humidity controlled rooms with a 12 hour light-dark cycle and allowed free access to chow and house distilled water.

Primary hepatocytes were isolated with a two-step collagen perfusion using methods described in detail elsewhere (Kocarek and Reddy, 1996; Wu et al., 2001). Immediately following isolation, 1.2 million (mouse) or 1.6 million (rat) viable hepatocytes per well were plated onto collagen-coated 6-well plates. Hepatocyte cultures were maintained in Williams' E medium supplemented with 0.25 U/ml insulin, 0.1 μM triamcinolone acetonide, 100 U/ml penicillin, and 100 μg/ml streptomycin. Twenty-four hours after plating, medium was replaced with fresh medium containing Matrigel (1 to 50 dilution). The following day, cholesterol synthesis inhibitors (0.1 μM SQ1 or 30 μM Prav) or nuclear receptor activators (100 μM PB, 0.25 μM TCPOBOP, or 100 μM Cipro) were added to the culture medium from concentrated

JPET Fast Forward. Published on May 25, 2016 as DOI: 10.1124/jpet.116.233312
This article has not been copyedited and formatted. The final version may differ from this version.

stock solutions dissolved in either water (SQ1, Prav, PB) or DMSO (TCPOBOP, Cipro). Culture medium containing drugs was replaced once after 24 h. Forty-eight hours following the initial treatment, total RNA was extracted from the hepatocytes and processed for microarray or *q*RT-PCR analysis as described in more detail below.

Microarrays of Mouse and Rat Hepatocytes Treated with SQ1 or Prav. Two independent preparations of primary cultured mouse or rat hepatocytes were treated with either medium alone (i.e., untreated control) or medium containing SQ1 or Prav (8 wells/treatment/hepatocyte preparation; 16 wells/treatment/species total). Forty-eight hours following the initial drug treatment, total RNA was extracted from the hepatocytes and column purified with RNeasy columns (Qiagen; Valencia, CA). Following isolation, RNA quality was assessed using a 2100 Bioanalyzer (Agilent Technologies; Santa Clara, CA) and only high quality RNA (RNA integrity number >9) was used in subsequent steps. Total RNA was pooled from two wells/treatment group, providing 8 RNA samples/treatment group/species for microarray analysis. The RNA samples (500 ng) with Agilent spike-in controls were amplified using the TargetAMP 1-Round Aminoallyl-aRNA Amplification Kit 101 according to manufacturers' instructions (Epicentre, Madison, WI). Five µg of each aminoallyl-aRNA sample was then fluorescently labeled with Alexa 647 or Alexa 555. Microarrays were performed using Mouse GE 4x44K v2 and Rat GE 4x44K v3 whole genome arrays (Agilent Technologies), with a basic two-color hybridization design to compare relative gene expression levels in SQ1 vs untreated (control) and Prav vs control samples. To minimize the potential effect of transcript-dependent dye bias on fluorescent intensity signals, for each set of 8 arrays, 4 of the arrays were hybridized with Alexa 647-labeled RNA from control samples and Alexa 555-labeled RNA from drug-treated samples, while in the

JPET Fast Forward. Published on May 25, 2016 as DOI: 10.1124/jpet.116.233312
This article has not been copyedited and formatted. The final version may differ from this version.

other 4 arrays the dye orientation was reversed. Microarrays were scanned using the Agilent dual laser DNA microarray scanner (Model G2565AA) and image analysis was performed using Agilent Feature Extraction software. Outlier features having aberrant image characteristics were flagged and excluded from subsequent analysis. The data were further processed and analyzed as described in detail within the Statistical Analyses section. All microarray data have been deposited and are available on the GEO database (www.ncbi.nlm.nih.gov/geo).

Quantitative Reverse Transcription Polymerase Chain Reaction (*q*RT-PCR). Forty-eight hours following the initial drug treatment, total RNA was extracted from cells, and cDNA was synthesized from total RNA (2 µg) using the High Capacity Reverse Transcription cDNA Kit (Life Technologies, Carlsbad, CA). Quantitative determination of gene expression was performed using the StepOne Plus Real Time PCR System (Applied Biosystems, Foster City, CA), gene-specific primers (75-250 nM), and SYBR green master mix. Primers were designed using the Primer-BLAST program (https://www.ncbi.nlm.nih.gov/tools/primer-blast/) (Ye et al., 2012), and a complete listing of the mouse and rat primer pairs used for gene expression analysis is available in **Supplemental Tables 1-2.** For each assay, a commercially designed primer set to detect mouse (P/N Mm.PT.39a.22214839) or rat (P/N Rn.PT.51.24118050) TATA binding protein (TBP) was purchased from Integrated DNA Technologies (IDT; Coralville, IA) and used as the endogenous control. The PCR cycling conditions have been described in detail elsewhere (Rondini et al., 2016). All assays were performed in duplicate (n=3-6/treatment) and the relative fold-changes were then quantitated using the comparative C_T ($\Delta\Delta C_T$) method.

JPET Fast Forward. Published on May 25, 2016 as DOI: 10.1124/jpet.116.233312
This article has not been copyedited and formatted. The final version may differ from this version.

Statistical Analyses. Statistical analysis for *q*RT-PCR was performed using SigmaStat Statistical Software (Version 3.5; Point Richmond, CA). Normalized expression values were analyzed using a one or two-way analysis of variance (ANOVA) as appropriate, and when significant differences were detected ($P<0.05$), group comparisons were made using the Student-Newman-Keuls test. Results are presented as mean ± S.E.M. For microarray analysis, raw fluorescence intensities were normalized using the Lowess method in Agilent's Feature Extraction Software (Santa Clara, CA). Normalized values were then imported into Genespring v 12.6.1 for further filtering and statistical analyses (Agilent; Santa Clara, CA). Differentially expressed transcripts (SQ1 vs untreated controls, Prav vs control, SQ1 vs Prav) were detected using a T-test against zero and the Benjamini & Hochberg False Discovery Rate (FDR) post-test to correct for multiple comparisons. Results were filtered to exclude genes with an FDR > 5% and those displaying less than a ± 1.5-fold change between treatments. Differentially expressed transcripts were then exported into Microsoft Excel and Access for further sorting and processing. When present, values from replicate transcripts were averaged. For inter-species comparisons, orthologous genes were retrieved using Homologene (http://www.ncbi.nlm.nih.gov/homologene) and the rat genome databases (http://rgd.mcw.edu/). The PANTHER database (http://www.pantherdb.org/) was used to classify transcripts into biological categories and the Web-based Gene Set Analysis Toolkit (http://bioinfo.vanderbilt.edu/webgestalt/option.php) for Pathway enrichment analysis. Pathway enrichment *P* values were calculated using a hypergeometric distribution test followed by the Benjamini & Hochberg post-test. Heat Maps displaying differential gene changes were generated using GENE-E software v 3.0.204

JPET Fast Forward. Published on May 25, 2016 as DOI: 10.1124/jpet.116.233312
This article has not been copyedited and formatted. The final version may differ from this version.

(http://www.broadinstitute.org/cancer/software/GENE-E/index.html) and data are displayed on a Log2 scale.

Results.

Profile of global gene expression changes significantly altered in primary cultured mouse and rat hepatocytes following treatment with SQ1 or Prav. The number and distribution of RNA transcripts significantly altered by either SQ1 or Prav in primary cultured mouse hepatocytes are presented in **Fig. 2**. Among the 39, 430 genes represented on the mouse Agilent microarray slides, 691 transcripts (318 upregulated and 373 downregulated) were significantly affected by SQ1 and 3567 transcripts by Prav (1433 upregulated, 2134 downregulated) when compared to untreated, control hepatocytes (**Fig. 2A**). Among these, 333 genes (166 upregulated, 167 downregulated) were unique to SQ1 treatment, 3209 genes (1303 up, 1906 down) were unique to Prav, and 358 genes were significantly affected by both treatments (111 co-upregulated, 188 co-downregulated, 59 differentially regulated; ≥1.5-fold, $P<0.05$; **Fig. 2B**). As shown in **Fig. 2C**, a large portion of the known genes significantly affected by either treatment were associated with metabolic (lipid, protein, nucleobase-containing) and cellular processes (cell communication, movement, and cell cycle), representing ~45% of the total gene expression changes.

RNA transcripts significantly affected in primary cultured rat hepatocytes are presented in **Fig. 2D.** Among the 30,003 Entrez gene probes represented on the rat arrays, 2803 transcripts (1196 upregulated and 1607 downregulated) were significantly affected by SQ1 and 943 transcripts by Prav (425 upregulated, 518 downregulated) compared to untreated controls (**Fig. 2D**). SQ1 treatment uniquely affected 2182 genes (888 upregulated, 1294 downregulated), Prav

JPET Fast Forward. Published on May 25, 2016 as DOI: 10.1124/jpet.116.233312
This article has not been copyedited and formatted. The final version may differ from this version.

affected 322 (126 upregulated, 196 downregulated), while 621 genes were commonly affected by both cholesterol synthesis inhibitors (294 co-upregulated, 308 co-downregulated, 19 differentially regulated; **Fig. 2E**). Similar to the effects observed in mouse hepatocytes, a large share of genes affected by either treatment were associated with metabolic and cellular processes, representing ~45% of total known gene changes (**Fig. 2F**).

Comparative ortholog analysis to identify conserved common and drug-specific gene expression changes in primary mouse and rat hepatocytes. Species-specific responses to pharmacological and toxicological agents are generally accepted and have been well-reported (Forgacs et al., 2013). To understand key biological pathways affected by isoprenoid accumulation that are conserved across species and that therefore likely represent core functions of isoprenoids on hepatocellular physiology, lists of regulated genes among species were further processed to identify treatment-specific orthologs, as depicted in **Fig. 3A**. To identify orthologs uniquely affected by SQ1 treatment, we evaluated 313 of the SQ1-regulated mouse genes with known orthologs (264 of the 333 genes originally identified as unique to SQ1 treatment (**Fig. 2B**) and 49 differentially regulated transcripts from the 358 genes originally identified as regulated by both SQ1 and Prav (**Fig. 2B**)) and 1561 SQ1-regulated rat genes with known orthologs (1552 of the 2182 genes originally identified as unique to SQ1 and 9 differentially regulated transcripts from the 621 genes originally identified to be regulated by both SQ1 and Prav) (**Fig. 3A**)). To identify those uniquely affected by Prav treatment, we evaluated 2295 Prav-regulated mouse genes with known orthologs (2246 of the 3209 genes originally identified as unique to Prav (**Fig. 2B**) and 49 genes differentially regulated by SQ1 and Prav) and 221 Prav-regulated rat genes (212 of the 322 genes originally identified as unique to Prav in **Fig. 2B** and 9 differentially

expressed transcripts). Differentially expressed transcripts (SQ1 vs CON compared to Prav vs CON) are defined as genes significantly affected by both SQ1 and Prav and therefore originally included in the intersection (**Fig. 2B, 2E**), but displaying the opposite direction of change. Orthologs significantly co-regulated by both SQ1 and Prav treatment (286 genes in mice and 435 genes in rat hepatocytes) were also evaluated to identify conserved, drug-independent gene expression changes responsive to cellular cholesterol depletion.

Orthologous genes commonly affected by both SQ1 and Prav in primary cultured mouse and rat hepatocytes. As shown in **Fig. 3A and 3B**, we identified 47 orthologous genes commonly affected by both SQ1 and Prav in mouse and rat primary hepatocytes. Among these, 42 genes showed similar responses in both species with 23 genes co-induced by cholesterol synthesis inhibition and 19 genes co-repressed (**Fig. 3B**). However, the overall magnitude of the co-induced genes was species-dependent, with rats generally having responses of up to ~10-fold greater than those observed in mice for the most highly induced genes. Among orthologs co-induced were several involved in cholesterol biosynthesis (*Cyp51, Hmgcr, Mvd, Lss, Idi1, Pmvk, Nsdhl, Tm7sf2,* and *Hsd17b7*), whereas those co-repressed were associated with chemokine signaling (*Ccl6, Ccl12*), adipogenesis (*Lpl, Slc2a4*), as well as sodium/bile acid transport (*Slc10a1*). Other co-induced genes include the proprotein convertase subtilisin/kexin type 9 (*Pcsk9*), which targets the LDL receptor for degradation (Horton et al., 2007); *Stard4*, a sterol-responsive gene which regulates cholesterol transport between organelles (Rodriguez-Agudo et al., 2008; Calderon-Dominguez et al., 2014); the transcription factor *Nfe2*; and *Scd2* (*Scd* in rats), which is involved in the synthesis of monounsaturated fatty acids.

JPET Fast Forward. Published on May 25, 2016 as DOI: 10.1124/jpet.116.233312
This article has not been copyedited and formatted. The final version may differ from this version.

Orthologous genes uniquely affected by SQ1 in primary cultured mouse and rat hepatocytes. A heatmap displaying orthologs unique to SQ1 treatment compared to untreated controls is displayed in **Fig. 3C**. Ninety orthologs were found to be unique to SQ1 treatment, with 72 genes (26 co-induced and 46 co-repressed; 80% of genes) displaying the same direction of change whereas 18 genes were differentially expressed in mouse when compared with rat hepatocytes. Previous studies have indicated that treatment with either an SSI or farnesol increased the expression of select PPAR-regulated genes (Takahashi et al., 2002; Goto et al., 2011b). Consistent with these findings, we found that many of the genes co-induced by SQ1 were strongly associated with lipid/fatty acid metabolism and are also identified as PPAR target genes including *Cyp4a10, Cyp4a14* (*CYP4A2 and 4A3* in rat), *Cyp4a31* and *Cyp4a32* (*CYP4A1* in rat), *Cpt1b*, and *Ehhadh*. Additional classes of genes co-induced included those involved in drug/xenobiotic metabolism [*Cyp2b10*, *Cyp2b23* (*CYP2B1/2* and *CYP2B21*, respectively in rat)] as well as several acyl-CoA thioesterases (*Acot1*, *Acot2*, *Acot3*, *Acot4*), which play a role in lipid metabolism by regulating intracellular CoA levels and levels of activated substrates for peroxisomal and mitochondrial fatty acid oxidation (Hunt et al., 2012; Hunt et al., 2014) (**Fig. 3C**). Among the genes uniquely co-repressed by SQ1-treated when compared to control hepatocytes were those involved in cell cycle regulation, including several cyclins (*Ccna2*, *Ccnb1*, *Ccnb2*, *Ccne2*), the cyclin dependent kinase *Cdk1*, and genes associated with DNA replication/chromosome segregation (*Orc1*, *Plk1*, and *Top2a*) (**Fig. 3C**).

Orthologous genes uniquely affected by Prav in primary cultured mouse and rat hepatocytes. A heatmap displaying orthologs unique to Prav treatment compared to untreated controls is displayed in **Fig. 3D**. A total of 51 orthologous genes were identified, among which 41 (9 co-induced and 32 co-repressed; 80% of genes) displayed the same direction of change

JPET Fast Forward. Published on May 25, 2016 as DOI: 10.1124/jpet.116.233312
This article has not been copyedited and formatted. The final version may differ from this version.

across species. A majority of the conserved genes specific for Prav treatment were co-repressed, including several involved in retinol and xenobiotic metabolism (*Adh1, Adh7, Cyp1a2, Ugtb1*) as well as in metabolic pathways (*Ces1e, Uroc1, Adh7, Gck, Gls2, Adh1, Csad*). Orthologs that were co-induced include the sterol-sensitive transcription factor sterol regulatory element-binding factor-2 (*Srebf2)*, epoxide hydrolase 4 (*Ephx4*), the iron-regulatory and type II acute phase protein hepcidin (*Hamp*), and the amyotrophic lateral sclerosis 2 gene (*Als2cr12*), which encodes a putative GTPase regulator (Hadano et al., 2001) (**Fig. 3D**).

Orthologous genes differentially affected by SQ1 compared to Prav in primary cultured mouse and rat hepatocytes. Obvious species-specific differences in the magnitude of fold-changes were observed following treatment with SQ1 or Prav, most notably for cholesterol biosynthetic enzymes (**Fig. 3B**). To gain further insight into effects that may have been more subtly regulated by isoprenoid depletion (Prav) or accumulation (SQ1) across species but are nonetheless important in isoprenoid signaling and physiology, we additionally compared orthologous expression between treatments (SQ1 vs Prav) using a 1.5-fold cut-off for biological significance.

As shown in **Fig. 4A**, we identified 3154 transcripts (1873 higher, 1281 lower) that were differentially affected in the mouse and 1652 (723 higher, 929 lower) in the rat when comparing SQ1- versus Prav-treated hepatocytes (**Fig. 4A**). Among these, 410 orthologs were affected in both species (**Fig. 4B, 4C**), whereas 1867 (mouse) and 780 (rat) orthologs exhibited species-specific expression patterns (**Fig. 4B**). Within the 410 orthologs that were commonly affected, 162 orthologs displayed similar expression patterns in both species (104 genes that were differentially higher and 58 differentially lower in SQ1-treated relative to Prav-treated

JPET Fast Forward. Published on May 25, 2016 as DOI: 10.1124/jpet.116.233312
This article has not been copyedited and formatted. The final version may differ from this version.

hepatocytes) (**Fig. 4B, 4C**). Orthologs that were differentially lower in SQ1-treated hepatocytes included several genes involved in cell cycle regulation (*Orc1, Cdc6, Pole2, Bub1b*) as well as cytokine signaling (*Tnf, Cd40, Ccl7, Tnfsf18, Kitl, Cxcl2*) (**Fig. 4C**). *Nr0b2*, the prototypical target gene for FXR activation was also differentially regulated by the treatments, being strongly repressed by Prav and more moderately reduced by SQ1. As observed when comparing SQ1 to controls, several genes that were differentially higher in SQ1-treated compared to Prav-treated hepatocytes included a cluster of PPAR-regulated genes [*Cyp4a10 (CYP4A1* in rat), *Fabp1, Acox1, Cpt1b, Cyp4a31 and 4a32 (CYP4A1* in rat), *Cyp4a14* (*CYP4A2 and 4A3* in rat), *Acaa1b, Acsl1, Cpt2,* and *Ehhadh*], and genes involved in fatty acid β-oxidation (*Cpt1b, Acat1, Ehhadh, Ech1, Hadh, Hadha, Hadhb, Decr1, Crat, Acsl1, Slc25a20, Cpt2, Abcd3*), fatty acid ω-oxidation (*Aldh1a1, Adh7, Cyp1a2*), drug and xenobiotic metabolism [*Cyp2b10* (*CYP2B1* in rat), *Cyp2b23* (*CYP2B21* in rat), *Cyp3a11* (*CYP3A23/3A1* in rat), *Cyp3a16* (*CYP3A23/3A1* in rat), *Adh7*, *Cyp1a2*, *Ugt2b1, Gstk1*)], as well as various ACOT enzymes such as *Acot1* (cytosolic), *Acot2* (mitochondrial), and *Acots 3, 4,* and *5* (peroxisomal).

Validation of select gene expression changes by *q*RT-PCR. The relative expression of several genes involved in cholesterogenesis and lipid metabolism in response to SQ1 and Prav treatment was further validated by *q*RT-PCR and results are presented in **Fig. 5-6**. In general, the expression changes observed using microarrays were in accordance with the changes measured by *q*RT-PCR. As shown in **Fig. 5A-B**, treatment with either drug, as expected, resulted in transcriptional upregulation of several cholesterol biosynthetic enzymes including *Hmgcs1, Hmgcr, Mvd, Idi1, Lss,* and *Cyp51*; however, the relative fold-changes were generally lower in

JPET Fast Forward. Published on May 25, 2016 as DOI: 10.1124/jpet.116.233312
This article has not been copyedited and formatted. The final version may differ from this version.

mouse hepatocytes (**Fig. 5A**) than those observed in rat hepatocytes (**Fig. 5B**), reflecting species differences in hepatocellular responses to cholesterol depletion.

Select genes differentially regulated by SQ1 and Prav were also analyzed by *q*RT-PCR (**Fig. 6A, 6B**). Since many of the differentially regulated transcripts were identified as putative PPAR- or CAR-target genes with identified roles in lipid and xenobiotic metabolism, respectively, we focused on orthologs within this cluster for further confirmation (**Fig. 6A, 6B**). As shown in **Fig. 6A** and **6B**, the prototypical PPAR and CAR target genes, *Cyp4a10* (*CYP4A1* in rats) and *Cyp2b10* (*CYP2B1* in rats), respectively, were strongly induced (>3-fold) by SQ1 across species, although CAR-mediated responses tended to be higher in rat hepatocytes whereas PPAR-mediated responses were greater in mouse hepatocytes (**Fig. 6A, 6B**). Genes associated with peroxisomal (*Acox1*, *Acot3*, *Acot4*, *Ehhadh*) and mitochondrial β-oxidation (*Acaa2*, *Acot2*, *Hadhb*, *Cpt1b*, *Cpt2*, *Slc25a20*) were also generally expressed at higher levels in SQ1- compared to Prav-treated hepatocytes. However, in the mouse, endogenous isoprenoids appeared to influence basal expression of these genes as Prav treatment downregulated their mRNA levels, while SQ1 either did not change or increased the mRNA levels compared to untreated hepatocytes (**Fig. 6A**). In comparison, in rat hepatocytes the expression levels were much less affected by Prav and generally induced following SQ1 treatment (**Fig. 6B**). Other genes differentially regulated by SQ1 included the mitochondrial solute transporter *Slc25a34*, the pyruvate dehydrogenase inhibitor *Pdk4*, liver fatty acid binding protein (*Fabp1*), *Aldh1a1*, an aldehyde dehydrogenase enzyme involved in ω-oxidation and retinol metabolism, as well as *Acsl1* and *Acot1*, which are enzymes involved in regulating activation and deactivation of fatty acids, respectively (**Fig. 6A-B**).

JPET Fast Forward. Published on May 25, 2016 as DOI: 10.1124/jpet.116.233312
This article has not been copyedited and formatted. The final version may differ from this version.

As shown in **Fig. 7A** and **B**, most of the metabolic enzymes that were surveyed were also inducible by the prototypical PPARα agonist, Cipro, in both species whereas Cipro-mediated induction of the mRNA for *Acaa2*, *Acsl1*, *Hadhb*, and *Slc25a20* was significant in rats only. Comparably, despite a suggested role for CAR in lipid metabolism in rodents, only *CYP2B* expression was induced by the prototypical CAR agonists TCPOBOP and PB in mouse and rat hepatocytes, respectively (**Fig. 7A, 7B**). A species-dependent interaction was also observed among treatments with respect to gene regulation by the nuclear receptors CAR and PPAR. These changes may reflect species-dependent regulation of CAR responses following PPAR activation as discussed elsewhere (Guo et al., 2006; Wieneke et al., 2007; Saito et al., 2010; Rondini et al., 2016). In mouse hepatocytes, PPAR activation by the prototypical agonist Cipro decreased expression of the CAR target gene, *Cyp2b10*, by ~50%, whereas in the rat, PPAR activation increased *CYP2B1* expression by ~5-fold. CAR activation in rat hepatocytes also partially suppressed expression of the PPAR target genes *Cyp4a1*, *Pdk4*, *Ehhadh*, *Cpt2*, and *Slc25a20*, but this effect was not observed in mouse hepatocytes (**Fig. 7A, B**).

Discussion.

The current investigation was designed to elucidate the effects of endogenous isoprenoids on gene expression in primary mouse and rat hepatocytes. Using microarrays, we compared orthologous gene expression produced by two cholesterol synthesis inhibitors: SQ1, which causes isoprenoid accumulation, and Prav, which blocks isoprenoid production. Although not the primary focus of this study, orthologs commonly affected by both cholesterol synthesis inhibitors

JPET Fast Forward. Published on May 25, 2016 as DOI: 10.1124/jpet.116.233312
This article has not been copyedited and formatted. The final version may differ from this version.

were also evaluated to differentiate the effects of sterol depletion from those due to isoprenoid accumulation.

Both statins and SSIs reduce non-HDL cholesterol by inhibiting *de novo* cholesterol biosynthesis, leading to a compensatory upregulation of LDL receptors on the surface of the hepatocytes and enhanced clearance of LDL-cholesterol (Bilheimer et al., 1983; Nishimoto et al., 2003). This transcriptional pathway is regulated through activation of the sterol regulatory element-binding proteins (SREBPs) (Horton et al., 2002). Under reduced sterol conditions, inactive SREBP precursors are transported from the endoplasmic reticulum to the Golgi apparatus for proteolytic processing, resulting in nuclear translocation and activation of responsive genes (Goldstein and Brown, 2015). In the current study, many of the orthologs co-induced by SQ1 and Prav have been previously identified as SREBP2 targets (Horton et al., 2003) and are consistent with changes identified in tissues of SREBP2-transgenic mice (Ma et al., 2014). For example, the most highly induced class of genes was associated with cholesterol and unsaturated fatty acid biosynthesis. The level of upregulation was similar between drugs, indicating comparable effects on cholesterol inhibition. However the most striking difference was in the magnitude of change across species. In general, the fold changes were several-fold higher in rat than in mouse hepatocytes. The basal hepatic cholesterol synthesis rate is reportedly 4-12 times higher in rats compared to other species (Spady and Dietschy, 1983), suggesting that this difference may influence the magnitude of SREBP2-mediated responses under conditions of reduced sterol synthesis.

SSIs markedly reduce triglyceride biosynthesis, which is independent from effects on LDL cholesterol (Hiyoshi et al., 2001; Amano et al., 2003) and is dependent on metabolism through the farnesol pathway (Hiyoshi et al., 2003). Isoprenoids are known to modulate nuclear

JPET Fast Forward. Published on May 25, 2016 as DOI: 10.1124/jpet.116.233312
This article has not been copyedited and formatted. The final version may differ from this version.

receptor signaling pathways including PPAR, CAR, and FXR (Forman et al., 1995; O'Brien et al., 1996; Kocarek and Mercer-Haines, 2002; Takahashi et al., 2002; Goto et al., 2011a), which is suggested to partially account for some of these effects (Goto et al., 2011a). In the current study, many of the orthologs uniquely affected by SQ1 treatment were associated with fatty acid metabolism and are also transcriptional targets of PPARα. Therefore, at least some of these gene expression changes are likely attributable to isoprenoid-mediated PPAR activation. The CAR-target gene, CYP2B, was also induced, although more strongly in rat than in mouse hepatocytes. Although CAR is suggested to influence hepatocellular lipid metabolism (Dong et al., 2009; Goto et al., 2011a), the panel of fatty acid-metabolizing enzymes altered by isoprenoids in this study did not appear to be strongly regulated through CAR activation.

The metabolic route for FPP metabolism following squalene synthase inhibition is proposed to occur through the farnesol–farnesoic acid–DCA pathway described by Gonzales-Pacanowska *et al.* (Gonzalez-Pacanowska et al., 1988), although an alternative pathway has been suggested (DeBarber et al., 2004). Farnesol-derived DCAs are then partially catabolized from the ω-carbon, producing a family of C_{12} and C_{10} DCAs that can be detected in the urine (Bostedor et al., 1997; Vaidya et al., 1998). The enzymatic steps involved in this pathway have not been fully elucidated; however, based on the gene expression changes observed in this study, they may involve components of microsomal, peroxisomal, as well as mitochondrial oxidation. For example, oxidation of farnesol to farnesoic acid was recently shown to be catalyzed by alcohol dehydrogenases 1 and 7 followed by a microsomal aldehyde dehydrogenase (Endo et al., 2011), and we found *Adh7* to be regulated by SQ1 treatment. Several *CYP4A* orthologs were also highly induced by SQ1 compared to control or Prav-treated cells. CYP4A enzymes catalyze the ω-hydroxylation of various fatty acid substrates (Okita and Okita, 2001), including the

branched fatty acid phytanic acid (Xu et al., 2006), and based on the extent of upregulation in this study may potentially be involved in catalyzing the ω-hydroxylation of farnesoic acid.

Peroxisomal β-oxidation is involved in chain length shortening of fatty acids and is the primary pathway for metabolism of bile acids, and very long chain and branched-chain fatty acids (Reddy and Hashimoto, 2001). In the current study, several genes associated with peroxisomal and mitochondrial β-oxidation were regulated by SQ1. Additionally, *Acot* genes were also upregulated following SQ1 treatment. ACOTs are auxiliary enzymes catalyzing the hydrolysis of fatty acyl-CoAs with suggested roles in regulating intracellular CoA levels and in fatty acid metabolism (Hunt and Alexson, 2008), potentially by generating ligands for PPAR activation (Gachon et al., 2011; Hunt et al., 2014). Many of these changes are consistent with farnesol-derived DCAs undergoing partial oxidation in the peroxisome, producing chain-shortened DCAs that can then either be excreted or further metabolized in the mitochondria (Hiyoshi et al., 2003). Based on substrate specificity, ACOT3 or ACOT5 (ACOT4 in humans) would likely terminate peroxisomal β-oxidation, producing the DCAs identified by Bostedor *et al*. (Bostedor et al., 1997), although additional steps involved in regulating the extent of oxidation and degree of saturation are not currently known. Building on previous findings and the SQ1-mediated gene expression changes detected in the current study, a proposed model of FPP metabolism is depicted in **Fig. 8**.

The most enriched gene class repressed by SQ1 when compared to either control or Prav-treated hepatocytes was associated with cell cycle regulation and DNA synthesis. These effects were not observed with Prav. Farnesol has been reported to induce apoptosis and cell cycle arrest in a number of different cell lines, with cancer cells more sensitive to the effects of farnesol (Wiseman et al., 2007; Joo and Jetten, 2010). Although SSIs had good hepatic safety in

JPET Fast Forward. Published on May 25, 2016 as DOI: 10.1124/jpet.116.233312
This article has not been copyedited and formatted. The final version may differ from this version.

preclinical trials (Nishimoto et al., 2003), Nagashima *et al.* (2015) recently described a transient liver dysfunction and mild hepatomegaly in hepatic-specific squalene synthase knockout mice (Nagashima et al., 2015). This was associated with elevated serum alanine aminotransferase levels and an increase in apoptotic and proliferative markers at a time point that coincided with higher farnesol production. Farnesol is hypothesized to be rapidly metabolized and difficult to detect even following treatment with SSI *in vivo* (Bergstrom et al., 1993; Vaidya et al., 1998). However, whether individual variations in the metabolic flux of FPP-derived isoprenoids could partially account for the hepatotoxicity that was observed in some individuals at the highest dose of TAK-475 (Stein et al., 2011) is worthy of future consideration.

Conserved gene expression changes unique to Prav treatment are likely secondary to depletion of the pool of isoprenoids available for protein prenylation and other signaling pathways. For example, Prav uniquely repressed genes involved in xenobiotic and retinol metabolism, some of which are regulated by the nuclear receptors CAR and PXR (Xie et al., 2000; Yoshinari et al., 2010). *Adh*1 and 7 were also lower in Prav-treated cells, and these have been identified as enzymes involved in metabolizing farnesol and geranylgeraniol to their aldehyde derivatives (Endo et al., 2011). Additionally, some genes associated with fatty acid oxidation tended to be repressed in Prav-treated mouse, but not rat, hepatocytes, suggesting a greater sensitivity of PPAR target genes to isoprenoid depletion in mice. Conversely, Prav treatment increased expression of several orthologs including a putative GTPase regulator (*Als2cr12*), iron regulatory peptide (*Hamp*), potassium channel protein (*Kcn*), and epoxide hydrolase 4 (*Ephx*), suggesting that their transcription is normally repressed by endogenous isoprenoids, although the mechanism underlying this regulation is currently unknown.

Squalene synthase plays a pivotal role in cholesterol biosynthesis by regulating the flux of mevalonate-derived intermediates used for either sterol synthesis or production of nonsterol isoprenoids (Do et al., 2009). The current study provides insight into some of the conserved effects of SSIs on hepatocellular gene expression. The most profound effect of SQ1 was induction of several PPARα-regulated genes associated with fatty acid oxidation, which may at least partially explain the suppressive effects of SSIs on triglyceride biosynthesis (Ugawa et al., 2000; Hiyoshi et al., 2003). SQ1 treatment also influenced CAR targets involved in drug metabolism, and repressed several orthologs associated with cell cycle regulation. Limitations to this study are that SQ1- and Prav-mediated effects on gene expression may not always correspond to changes in protein levels or enzyme activities, and that the drug effects do not identify which specific isoprenoids mediate individual gene changes. Also, although we are unaware of evidence that Prav and SQ1 have any pharmacological targets other than HMGCR and squalene synthase, respectively, it remains possible that some effects on gene expression could have been produced by an off-target mechanism(s). Additional studies are needed to address the functional role(s) of identified gene expression changes on hepatocellular physiology. Notwithstanding these limitations, as there is continued interest in SSIs and the isoprenoid pathway (Goto et al., 2011a; Ichikawa et al., 2013; Nagashima et al., 2015; Saito et al., 2015), our findings provide a contextual framework for more mechanistic studies.

Acknowledgements.

The authors thank Mary Garagano for isolating the primary hepatocytes. We also thank Dr. Masahiko Negishi (National Institute of Environmental Health Sciences; Research Triangle Park, North Carolina) for providing the breeding mice that were essential to this study.

Authorship Contributions.

Participated in research design: Rondini, Kocarek, Dombkowski

Conducted experiments: Rondini, Duniec-Dmuchowski, Cukovic

Performed data analysis: Rondini, Dombkowski

Wrote or contributed to the writing of the manuscript: Rondini, Kocarek

References.

Amano Y, Nishimoto T, Tozawa R, Ishikawa E, Imura Y and Sugiyama Y (2003) Lipid-lowering effects of TAK-475, a squalene synthase inhibitor, in animal models of familial hypercholesterolemia. *European journal of pharmacology* **466**:155-161.

Bergstrom JD, Kurtz MM, Rew DJ, Amend AM, Karkas JD, Bostedor RG, Bansal VS, Dufresne C, VanMiddlesworth FL, Hensens OD and et al. (1993) Zaragozic acids: a family of fungal metabolites that are picomolar competitive inhibitors of squalene synthase. *Proceedings of the National Academy of Sciences of the United States of America* **90**:80-84.

Bilheimer DW, Grundy SM, Brown MS and Goldstein JL (1983) Mevinolin and colestipol stimulate receptor-mediated clearance of low density lipoprotein from plasma in familial hypercholesterolemia heterozygotes. *Proceedings of the National Academy of Sciences of the United States of America* **80**:4124-4128.

Bostedor RG, Karkas JD, Arison BH, Bansal VS, Vaidya S, Germershausen JI, Kurtz MM and Bergstrom JD (1997) Farnesol-derived dicarboxylic acids in the urine of animals treated with zaragozic acid A or with farnesol. *The Journal of biological chemistry* **272**:9197-9203.

Boullart AC, de Graaf J and Stalenhoef AF (2012) Serum triglycerides and risk of cardiovascular disease. *Biochimica et biophysica acta* **1821**:867-875.

Calderon-Dominguez M, Gil G, Medina MA, Pandak WM and Rodriguez-Agudo D (2014) The StarD4 subfamily of steroidogenic acute regulatory-related lipid transfer (START)

domain proteins: new players in cholesterol metabolism. *The international journal of biochemistry & cell biology* **49**:64-68.

Campbell CY, Rivera JJ and Blumenthal RS (2007) Residual risk in statin-treated patients: future therapeutic options. *Current cardiology reports* **9**:499-505.

Cholesterol Treatment Trialists C, Baigent C, Blackwell L, Emberson J, Holland LE, Reith C, Bhala N, Peto R, Barnes EH, Keech A, Simes J and Collins R (2010) Efficacy and safety of more intensive lowering of LDL cholesterol: a meta-analysis of data from 170,000 participants in 26 randomised trials. *Lancet* **376**:1670-1681.

Cholesterol Treatment Trialists C, Fulcher J, O'Connell R, Voysey M, Emberson J, Blackwell L, Mihaylova B, Simes J, Collins R, Kirby A, Colhoun H, Braunwald E, La Rosa J, Pedersen TR, Tonkin A, Davis B, Sleight P, Franzosi MG, Baigent C and Keech A (2015) Efficacy and safety of LDL-lowering therapy among men and women: meta-analysis of individual data from 174,000 participants in 27 randomised trials. *Lancet* **385**:1397-1405.

Dallner G and Sindelar PJ (2000) Regulation of ubiquinone metabolism. *Free radical biology & medicine* **29**:285-294.

DeBarber AE, Bleyle LA, Roullet JB and Koop DR (2004) Omega-hydroxylation of farnesol by mammalian cytochromes p450. *Biochimica et biophysica acta* **1682**:18-27.

Do R, Kiss RS, Gaudet D and Engert JC (2009) Squalene synthase: a critical enzyme in the cholesterol biosynthesis pathway. *Clinical genetics* **75**:19-29.

Dong B, Saha PK, Huang W, Chen W, Abu-Elheiga LA, Wakil SJ, Stevens RD, Ilkayeva O, Newgard CB, Chan L and Moore DD (2009) Activation of nuclear receptor CAR

ameliorates diabetes and fatty liver disease. *Proceedings of the National Academy of Sciences of the United States of America* **106**:18831-18836.

Duncan RE and Archer MC (2008) Farnesol decreases serum triglycerides in rats: identification of mechanisms including up-regulation of PPARalpha and down-regulation of fatty acid synthase in hepatocytes. *Lipids* **43**:619-627.

Eckel RH, Grundy SM and Zimmet PZ (2005) The metabolic syndrome. *Lancet* **365**:1415-1428.

Edwards PA and Ericsson J (1999) Sterols and isoprenoids: signaling molecules derived from the cholesterol biosynthetic pathway. *Annual review of biochemistry* **68**:157-185.

Endo S, Matsunaga T, Ohta C, Soda M, Kanamori A, Kitade Y, Ohno S, Tajima K, El-Kabbani O and Hara A (2011) Roles of rat and human aldo-keto reductases in metabolism of farnesol and geranylgeraniol. *Chemico-biological interactions* **191**:261-268.

Forgacs AL, Dere E, Angrish MM and Zacharewski TR (2013) Comparative analysis of temporal and dose-dependent TCDD-elicited gene expression in human, mouse, and rat primary hepatocytes. *Toxicological sciences : an official journal of the Society of Toxicology* **133**:54-66.

Forman BM, Goode E, Chen J, Oro AE, Bradley DJ, Perlmann T, Noonan DJ, Burka LT, McMorris T, Lamph WW, Evans RM and Weinberger C (1995) Identification of a nuclear receptor that is activated by farnesol metabolites. *Cell* **81**:687-693.

Gachon F, Leuenberger N, Claudel T, Gos P, Jouffe C, Fleury Olela F, de Mollerat du Jeu X, Wahli W and Schibler U (2011) Proline- and acidic amino acid-rich basic leucine zipper proteins modulate peroxisome proliferator-activated receptor alpha (PPARalpha) activity. *Proceedings of the National Academy of Sciences of the United States of America* **108**:4794-4799.

Goldstein JL and Brown MS (2015) A Century of Cholesterol and Coronaries: From Plaques to Genes to Statins. *Cell* **161**:161-172.

Gonzalez-Pacanowska D, Arison B, Havel CM and Watson JA (1988) Isopentenoid synthesis in isolated embryonic Drosophila cells. Farnesol catabolism and omega-oxidation. *The Journal of biological chemistry* **263**:1301-1306.

Goto T, Kim YI, Funakoshi K, Teraminami A, Uemura T, Hirai S, Lee JY, Makishima M, Nakata R, Inoue H, Senju H, Matsunaga M, Horio F, Takahashi N and Kawada T (2011a) Farnesol, an isoprenoid, improves metabolic abnormalities in mice via both PPARalpha-dependent and -independent pathways. *American journal of physiology Endocrinology and metabolism* **301**:E1022-1032.

Goto T, Nagai H, Egawa K, Kim YI, Kato S, Taimatsu A, Sakamoto T, Ebisu S, Hohsaka T, Miyagawa H, Murakami S, Takahashi N and Kawada T (2011b) Farnesyl pyrophosphate regulates adipocyte functions as an endogenous PPARgamma agonist. *The Biochemical journal* **438**:111-119.

Guo D, Sarkar J, Ahmed MR, Viswakarma N, Jia Y, Yu S, Sambasiva Rao M and Reddy JK (2006) Peroxisome proliferator-activated receptor (PPAR)-binding protein (PBP) but not PPAR-interacting protein (PRIP) is required for nuclear translocation of constitutive androstane receptor in mouse liver. *Biochemical and biophysical research communications* **347**:485-495.

Hadano S, Hand CK, Osuga H, Yanagisawa Y, Otomo A, Devon RS, Miyamoto N, Showguchi-Miyata J, Okada Y, Singaraja R, Figlewicz DA, Kwiatkowski T, Hosler BA, Sagie T, Skaug J, Nasir J, Brown RH, Jr., Scherer SW, Rouleau GA, Hayden MR and Ikeda JE

(2001) A gene encoding a putative GTPase regulator is mutated in familial amyotrophic lateral sclerosis 2. *Nature genetics* **29**:166-173.

Hafner M, Juvan P, Rezen T, Monostory K, Pascussi JM and Rozman D (2011) The human primary hepatocyte transcriptome reveals novel insights into atorvastatin and rosuvastatin action. *Pharmacogenetics and genomics* **21**:741-750.

Hatanaka T (2000) Clinical pharmacokinetics of pravastatin: mechanisms of pharmacokinetic events. *Clinical pharmacokinetics* **39**:397-412.

Healey GD, Collier C, Griffin S, Schuberth HJ, Sandra O, Smith DG, Mahan S, Dieuzy-Labaye I and Sheldon IM (2016) Mevalonate Biosynthesis Intermediates Are Key Regulators of Innate Immunity in Bovine Endometritis. *Journal of immunology* **196**:823-831.

Hiyoshi H, Yanagimachi M, Ito M, Ohtsuka I, Yoshida I, Saeki T and Tanaka H (2000) Effect of ER-27856, a novel squalene synthase inhibitor, on plasma cholesterol in rhesus monkeys: comparison with 3-hydroxy-3-methylglutaryl-coa reductase inhibitors. *Journal of lipid research* **41**:1136-1144.

Hiyoshi H, Yanagimachi M, Ito M, Saeki T, Yoshida I, Okada T, Ikuta H, Shinmyo D, Tanaka K, Kurusu N and Tanaka H (2001) Squalene synthase inhibitors reduce plasma triglyceride through a low-density lipoprotein receptor-independent mechanism. *European journal of pharmacology* **431**:345-352.

Hiyoshi H, Yanagimachi M, Ito M, Yasuda N, Okada T, Ikuta H, Shinmyo D, Tanaka K, Kurusu N, Yoshida I, Abe S, Saeki T and Tanaka H (2003) Squalene synthase inhibitors suppress triglyceride biosynthesis through the farnesol pathway in rat hepatocytes. *Journal of lipid research* **44**:128-135.

Horton JD, Cohen JC and Hobbs HH (2007) Molecular biology of PCSK9: its role in LDL metabolism. *Trends in biochemical sciences* **32**:71-77.

Horton JD, Goldstein JL and Brown MS (2002) SREBPs: activators of the complete program of cholesterol and fatty acid synthesis in the liver. *The Journal of clinical investigation* **109**:1125-1131.

Horton JD, Shah NA, Warrington JA, Anderson NN, Park SW, Brown MS and Goldstein JL (2003) Combined analysis of oligonucleotide microarray data from transgenic and knockout mice identifies direct SREBP target genes. *Proceedings of the National Academy of Sciences of the United States of America* **100**:12027-12032.

Hunt MC and Alexson SE (2008) Novel functions of acyl-CoA thioesterases and acyltransferases as auxiliary enzymes in peroxisomal lipid metabolism. *Progress in lipid research* **47**:405-421.

Hunt MC, Siponen MI and Alexson SE (2012) The emerging role of acyl-CoA thioesterases and acyltransferases in regulating peroxisomal lipid metabolism. *Biochimica et biophysica acta* **1822**:1397-1410.

Hunt MC, Tillander V and Alexson SE (2014) Regulation of peroxisomal lipid metabolism: the role of acyl-CoA and coenzyme A metabolizing enzymes. *Biochimie* **98**:45-55.

Ichikawa M, Ohtsuka M, Ohki H, Ota M, Haginoya N, Itoh M, Shibata Y, Ishigai Y, Terayama K, Kanda A and Sugita K (2013) Discovery of DF-461, a Potent Squalene Synthase Inhibitor. *ACS medicinal chemistry letters* **4**:932-936.

Joo JH and Jetten AM (2010) Molecular mechanisms involved in farnesol-induced apoptosis. *Cancer letters* **287**:123-135.

Kocarek TA, Dahn MS, Cai H, Strom SC and Mercer-Haines NA (2002) Regulation of CYP2B6 and CYP3A expression by hydroxymethylglutaryl coenzyme A inhibitors in primary cultured human hepatocytes. *Drug metabolism and disposition: the biological fate of chemicals* **30**:1400-1405.

Kocarek TA and Mercer-Haines NA (2002) Squalestatin 1-inducible expression of rat CYP2B: evidence that an endogenous isoprenoid is an activator of the constitutive androstane receptor. *Molecular pharmacology* **62**:1177-1186.

Kocarek TA and Reddy AB (1996) Regulation of cytochrome P450 expression by inhibitors of hydroxymethylglutaryl-coenzyme A reductase in primary cultured rat hepatocytes and in rat liver. *Drug metabolism and disposition: the biological fate of chemicals* **24**:1197-1204.

Krag SS (1998) The importance of being dolichol. *Biochemical and biophysical research communications* **243**:1-5.

Krisans SK, Ericsson J, Edwards PA and Keller GA (1994) Farnesyl-diphosphate synthase is localized in peroxisomes. *The Journal of biological chemistry* **269**:14165-14169.

Leszczynska A, Gora M, Plochocka D, Hoser G, Szkopinska A, Koblowska M, Iwanicka-Nowicka R, Kotlinski M, Rawa K, Kiliszek M and Burzynska B (2011) Different statins produce highly divergent changes in gene expression profiles of human hepatoma cells: a pilot study. *Acta biochimica Polonica* **58**:635-639.

Ma K, Malhotra P, Soni V, Hedroug O, Annaba F, Dudeja A, Shen L, Turner JR, Khramtsova EA, Saksena S, Dudeja PK, Gill RK and Alrefai WA (2014) Overactivation of intestinal SREBP2 in mice increases serum cholesterol. *PloS one* **9**:e84221.

Mathers CD, Boerma T and Ma Fat D (2009) Global and regional causes of death. *British medical bulletin* **92**:7-32.

McTaggart SJ (2006) Isoprenylated proteins. *Cellular and molecular life sciences : CMLS* **63**:255-267.

Nagashima S, Yagyu H, Tozawa R, Tazoe F, Takahashi M, Kitamine T, Yamamuro D, Sakai K, Sekiya M, Okazaki H, Osuga J, Honda A and Ishibashi S (2015) Plasma cholesterol-lowering and transient liver dysfunction in mice lacking squalene synthase in the liver. *Journal of lipid research* **56**:998-1005.

Nishimoto T, Amano Y, Tozawa R, Ishikawa E, Imura Y, Yukimasa H and Sugiyama Y (2003) Lipid-lowering properties of TAK-475, a squalene synthase inhibitor, in vivo and in vitro. *British journal of pharmacology* **139**:911-918.

O'Brien ML, Rangwala SM, Henry KW, Weinberger C, Crick DC, Waechter CJ, Feller DR and Noonan DJ (1996) Convergence of three steroid receptor pathways in the mediation of nongenotoxic hepatocarcinogenesis. *Carcinogenesis* **17**:185-190.

Okita RT and Okita JR (2001) Cytochrome P450 4A fatty acid omega hydroxylases. *Current drug metabolism* **2**:265-281.

Pant A and Kocarek TA (2016) Role of Phosphatidic Acid Phosphatase Domain Containing 2 in Squalestatin 1-Mediated Activation of the Constitutive Androstane Receptor in Primary Cultured Rat Hepatocytes. *Drug metabolism and disposition: the biological fate of chemicals* **44**:352-355.

Reddy JK and Hashimoto T (2001) Peroxisomal beta-oxidation and peroxisome proliferator-activated receptor alpha: an adaptive metabolic system. *Annual review of nutrition* **21**:193-230.

Rodriguez-Agudo D, Ren S, Wong E, Marques D, Redford K, Gil G, Hylemon P and Pandak WM (2008) Intracellular cholesterol transporter StarD4 binds free cholesterol and increases cholesteryl ester formation. *Journal of lipid research* **49**:1409-1419.

Rondini EA, Duniec-Dmuchowski Z and Kocarek TA (2016) Nonsterol Isoprenoids Activate Human Constitutive Androstane Receptor in an Isoform-Selective Manner in Primary Cultured Mouse Hepatocytes. *Drug metabolism and disposition: the biological fate of chemicals* **44**:595-604.

Saito K, Kobayashi K, Mizuno Y, Fukuchi Y, Furihata T and Chiba K (2010) Peroxisome proliferator-activated receptor alpha (PPARalpha) agonists induce constitutive androstane receptor (CAR) and cytochrome P450 2B in rat primary hepatocytes. *Drug metabolism and pharmacokinetics* **25**:108-111.

Saito K, Shirasago Y, Suzuki T, Aizaki H, Hanada K, Wakita T, Nishijima M and Fukasawa M (2015) Targeting cellular squalene synthase, an enzyme essential for cholesterol biosynthesis, is a potential antiviral strategy against hepatitis C virus. *Journal of virology* **89**:2220-2232.

Sampson UK, Fazio S and Linton MF (2012) Residual cardiovascular risk despite optimal LDL cholesterol reduction with statins: the evidence, etiology, and therapeutic challenges. *Current atherosclerosis reports* **14**:1-10.

Schroder A, Wollnik J, Wrzodek C, Drager A, Bonin M, Burk O, Thomas M, Thasler WE, Zanger UM and Zell A (2011) Inferring statin-induced gene regulatory relationships in primary human hepatocytes. *Bioinformatics* **27**:2473-2477.

Shang N, Li Q, Ko TP, Chan HC, Li J, Zheng Y, Huang CH, Ren F, Chen CC, Zhu Z, Galizzi M, Li ZH, Rodrigues-Poveda CA, Gonzalez-Pacanowska D, Veiga-Santos P, de Carvalho

TM, de Souza W, Urbina JA, Wang AH, Docampo R, Li K, Liu YL, Oldfield E and Guo RT (2014) Squalene synthase as a target for Chagas disease therapeutics. *PLoS pathogens* **10**:e1004114.

Spady DK and Dietschy JM (1983) Sterol synthesis in vivo in 18 tissues of the squirrel monkey, guinea pig, rabbit, hamster, and rat. *Journal of lipid research* **24**:303-315.

Stein EA, Bays H, O'Brien D, Pedicano J, Piper E and Spezzi A (2011) Lapaquistat acetate: development of a squalene synthase inhibitor for the treatment of hypercholesterolemia. *Circulation* **123**:1974-1985.

Takahashi N, Kawada T, Goto T, Yamamoto T, Taimatsu A, Matsui N, Kimura K, Saito M, Hosokawa M, Miyashita K and Fushiki T (2002) Dual action of isoprenols from herbal medicines on both PPARgamma and PPARalpha in 3T3-L1 adipocytes and HepG2 hepatocytes. *FEBS letters* **514**:315-322.

Tomaszewski M, Stepien KM, Tomaszewska J and Czuczwar SJ (2011) Statin-induced myopathies. *Pharmacological reports : PR* **63**:859-866.

Ugawa T, Kakuta H, Moritani H, Matsuda K, Ishihara T, Yamaguchi M, Naganuma S, Iizumi Y and Shikama H (2000) YM-53601, a novel squalene synthase inhibitor, reduces plasma cholesterol and triglyceride levels in several animal species. *British journal of pharmacology* **131**:63-70.

Vaidya S, Bostedor R, Kurtz MM, Bergstrom JD and Bansal VS (1998) Massive production of farnesol-derived dicarboxylic acids in mice treated with the squalene synthase inhibitor zaragozic acid A. *Archives of biochemistry and biophysics* **355**:84-92.

van Roermund CW, Ijlst L, Wagemans T, Wanders RJ and Waterham HR (2014) A role for the human peroxisomal half-transporter ABCD3 in the oxidation of dicarboxylic acids. *Biochimica et biophysica acta* **1841**:563-568.

Wieneke N, Hirsch-Ernst KI, Kuna M, Kersten S and Puschel GP (2007) PPARalpha-dependent induction of the energy homeostasis-regulating nuclear receptor NR1i3 (CAR) in rat hepatocytes: potential role in starvation adaptation. *FEBS letters* **581**:5617-5626.

Wiseman DA, Werner SR and Crowell PL (2007) Cell cycle arrest by the isoprenoids perillyl alcohol, geraniol, and farnesol is mediated by p21(Cip1) and p27(Kip1) in human pancreatic adenocarcinoma cells. *The Journal of pharmacology and experimental therapeutics* **320**:1163-1170.

Wu W, Kocarek TA and Runge-Morris M (2001) Sex-dependent regulation by dexamethasone of murine hydroxysteroid sulfotransferase gene expression. *Toxicology letters* **119**:235-246.

Xie W, Barwick JL, Downes M, Blumberg B, Simon CM, Nelson MC, Neuschwander-Tetri BA, Brunt EM, Guzelian PS and Evans RM (2000) Humanized xenobiotic response in mice expressing nuclear receptor SXR. *Nature* **406**:435-439.

Xu F, Ng VY, Kroetz DL and de Montellano PR (2006) CYP4 isoform specificity in the omega-hydroxylation of phytanic acid, a potential route to elimination of the causative agent of Refsum's disease. *The Journal of pharmacology and experimental therapeutics* **318**:835-839.

Yang YF, Jan YH, Liu YP, Yang CJ, Su CY, Chang YC, Lai TC, Chiou J, Tsai HY, Lu J, Shen CN, Shew JY, Lu PJ, Lin YF, Huang MS and Hsiao M (2014) Squalene synthase induces

tumor necrosis factor receptor 1 enrichment in lipid rafts to promote lung cancer metastasis. *American journal of respiratory and critical care medicine* **190**:675-687.

Ye J, Coulouris G, Zaretskaya I, Cutcutache I, Rozen S and Madden TL (2012) Primer-BLAST: a tool to design target-specific primers for polymerase chain reaction. *BMC bioinformatics* **13**:134.

Yoshinari K, Yoda N, Toriyabe T and Yamazoe Y (2010) Constitutive androstane receptor transcriptionally activates human CYP1A1 and CYP1A2 genes through a common regulatory element in the 5'-flanking region. *Biochemical pharmacology* **79**:261-269.

Footnotes.

Dr. Rondini was funded in part through a post-doctoral fellowship awarded through the Office of Vice President of Research (Wayne State University, Detroit, MI). This research was supported by the National Institutes of Health National Heart, Lung, and Blood Institute [Grant R01 HL050710] and National Institutes of Health National Institute of Environmental Health Sciences [Center Grant P30 ES020957].

JPET Fast Forward. Published on May 25, 2016 as DOI: 10.1124/jpet.116.233312
This article has not been copyedited and formatted. The final version may differ from this version.

Figure Legends.

Figure 1. Overview of the cholesterol biosynthetic pathway. Cholesterol synthesis inhibitors and their enzymatic targets are indicated. ***Abbreviations*:** *CYP51*, lanosterol 14α-demethylase; FPP, farnesyl pyrophosphate; *FPPS*, farnesyl pyrophosphate synthase; GGPP, geranylgeranyl pyrophosphate; *GGPPS*, geranylgeranyl pyrophosphate synthase; *HMGCR*, 3-hydroxy-3-methylglutaryl coenzyme A (CoA) reductase; *HMGCS1*, 3-hydroxy-3-methylglutaryl coenzyme A (CoA) synthase 1; *IDI1/2*, isopentenyl-diphosphate delta isomerase 1 and 2; *LSS*, lanosterol synthase; *MVD*, mevalonate diphosphate decarboxylase; *MVK*, mevalonate kinase; *PMVK*, phosphomevalonate kinase; *SQS*, squalene synthase; *SQE*, squalene epoxidase.

Figure 2. Characterization of gene expression changes in primary cultured mouse (A-C) and rat (D-F) hepatocytes following treatment with SQ1 or pravastatin identified using microarrays. Primary mouse and rat hepatocytes were freshly isolated and plated onto 6-well plates as described in the Materials and Methods. Forty eight hours following initial plating, hepatocytes were treated with Williams' E medium either alone (CON) or containing SQ1 (0.1 μM) or pravastatin (30 μM). Culture medium was replaced once after 24 h. Forty eight hours following the initial drug treatment, total RNA was isolated from hepatocytes and fluorescent-labeled RNA was synthesized and hybridized onto Agilent whole genome microarrays as described in the Materials and Methods (n=8/treatment group/species). Significant differences in the normalized fluorescence intensities (≥1.5-fold) among the different drug treatments (SQ1 vs CON, pravastatin vs CON) were detected using GeneSpring. (A, D) The total number of transcripts significantly affected by either SQ1 or pravastatin in mouse (A) and rat (B)

hepatocytes. (B, E) Venn diagrams displaying the number of common and unique transcripts significantly affected among the different drug treatments in mouse (B) and rat (E) hepatocytes. (C, F) Functional distribution of known gene changes from mouse (C) and rat (F) hepatocytes grouped into biological categories. Data are presented as percentage of total gene changes.

Figure 3. Orthologous genes affected by both SQ1 and Prav treatment in primary cultured mouse and rat hepatocytes identified using microarrays. Treatment-specific orthologs were retrieved using Homologene and the rat genome database as described in the Materials and Methods. (A) Venn diagram displaying the number of putative orthologs that were significantly affected by either SQ1 alone, both SQ1 and Prav, or Prav alone in mouse (upper panel) and rat hepatocytes (middle panel) and used to screen for conserved gene changes. The lower panel displays the number of treatment-specific orthologs that were commonly and uniquely affected in both species. (B-D) Heatmaps displaying the normalized (Log2) expression values of orthologs (B) commonly affected by both SQ1 and Prav, (C) unique to SQ1-treated hepatocytes, and (D) unique to Prav-treated hepatocytes (n=8/treatment group/species). When ortholog names differed between species, the mouse name is provided first followed by the rat name. Blue colored bars indicate upregulated genes and red colored bars indicate downregulated genes.

Figure 4. Hepatic expression of orthologs differentially affected by SQ1 compared to Prav in primary cultured mouse and rat hepatocytes identified using microarrays. Treatment-specific orthologs were retrieved using Homologene and the rat genome database as described in the Materials and Methods. (A) The total number of transcripts differentially affected in SQ1- compared to Prav-treated mouse and rat hepatocytes. (B) Venn diagram displaying the number

JPET Fast Forward. Published on May 25, 2016 as DOI: 10.1124/jpet.116.233312
This article has not been copyedited and formatted. The final version may differ from this version.

of orthologs differentially affected by SQ1 compared to Prav treatment (≥1.5-fold) in primary cultured mouse and rat primary hepatocytes. (C) A heatmap displaying the normalized (Log2) expression values of orthologs differentially expressed in SQ1 compared to Prav-treated hepatocytes from primary mouse and rat hepatocytes (n=8/treatment group/species). When ortholog names differed between species, the mouse name is provided first followed by the rat name. Blue colored bars indicate upregulated genes and red colored bars indicate downregulated genes.

Figure 5. Effect of SQ1 and pravastatin on the mRNA expression of cholesterol biosynthetic enzymes in primary cultured mouse (A) and rat (B) hepatocytes using *q*RT-PCR. Primary mouse (A) and rat (B) hepatocytes were freshly isolated, plated onto 6-well plates, and 48 h later treated with Williams' E medium either alone (CON) or containing SQ1 (0.1 μM) or Prav (30 μM). Medium was replaced once after 24 h, and 48 h after the initial treatment, cDNA was synthesized from total RNA as described in the Material and Methods. Relative changes in mRNA expression levels were quantified using *q*RT-PCR. Each bar represents the normalized values (mean ± SEM) from 5-6 hepatocyte preparations (2 combined wells/treatment group/preparation). *, Significant compared to untreated (CON) hepatocytes ($P<0.05$). δ, Significantly different compared to pravastatin-treated hepatocytes ($P<0.05$).

Figure 6. Validation of select regulated genes identified through microarrays by *q*RT-PCR in primary cultured mouse (A) and rat (B) hepatocytes. Primary mouse (A) and rat (B) hepatocytes were freshly isolated, plated onto 6-well plates, and 48 h later treated with Williams' E medium either alone (CON) or containing SQ1 (0.1 μM) or Prav (30 μM). Medium was

replaced once after 24 h, and 48 h after the initial treatment, total RNA was isolated and cDNA synthesized as described in the Materials and Methods. Relative changes in mRNA expression levels were determined using *q*RT-PCR. Each bar represents the normalized values (mean ± SEM) from 5-6 hepatocyte preparations (2 combined wells/treatment group/preparation). *, Significant compared to untreated (CON) hepatocytes ($P<0.05$). δ, Significantly different compared to Prav-treated hepatocytes ($P<0.05$).

Figure 7. Effects of nuclear receptor activators on the mRNA levels of select target genes in primary cultured mouse (A) and rat (B) hepatocytes. Primary mouse (A) and rat (B) hepatocytes were freshly isolated, plated onto 6-well plates, and after 48 h treated with Williams' E medium either alone (CON) or containing DMSO (0.1%), the PPAR-activator, Cipro (100 μM), or one of the CAR activators, TCPOBOP (0.25 μM, mouse) or PB (100 μM, rats). Medium was replaced once after 24 h, and 48 h after the initial treatment, total RNA was extracted from hepatocytes and used to synthesize cDNA as described in the Materials and Methods. Relative changes in mRNA levels were determined using *q*RT-PCR. Each bar represents the normalized values (mean ± SEM) from 3-4 hepatocyte preparations (2 combined wells/treatment group/preparation). *, Significant compared to untreated (CON) hepatocytes ($P<0.05$). †, Significantly different compared to DMSO-treated hepatocytes ($P<0.05$).

Figure 8. Proposed pathway of FPP metabolism following squalene synthase inhibition. Enzymes involved in the cholesterol biosynthetic pathway are localized to different subcellular compartments, with the production of FPP from mevalonate occurring in peroxisomes (Krisans et al., 1994). FPP is used either for the production of squalene by squalene synthase (SQS) or for

JPET Fast Forward. Published on May 25, 2016 as DOI: 10.1124/jpet.116.233312
This article has not been copyedited and formatted. The final version may differ from this version.

the synthesis of nonsterol isoprenoids. In the presence of squalene synthase inhibitors (SSI), FPP accumulates and is thought to be metabolized primarily through the farnesol–farnesoic acid–dicarboxylic acid (DCA) pathway (Gonzalez-Pacanowska et al., 1988). Farnesol-derived DCAs are then partially oxidized from the ω-carbon, producing chain-shortened (C_{12}, C_{10}) DCAs that are detectable in the urine (Bostedor et al., 1997; Vaidya et al., 1998). The enzymes involved in FPP catabolism have not been fully elucidated; however based on mRNA gene expression changes observed following SQ1 treatment in the current study, probably involve components of microsomal, peroxisomal, and mitochondrial oxidation. Shown is a proposed model of FPP catabolism in the presence of squalene synthase inhibitors, which extends on findings from others (Gonzalez-Pacanowska et al., 1988; Bergstrom et al., 1993; Endo et al., 2011; Pant and Kocarek, 2016). FPP can be dephosphorylated by phosphatidic acid phosphatase domain containing 2 (PPAPDC2) to produce farnesol, which is then sequentially oxidized to farnesal and then farnesoic acid. ADH1 and 7 were recently identified to catalyze the first oxidation step whereas ALDH3A2 was proposed to catalyze the second (Endo et al., 2011), although ALDH1A1 is another possible candidate based on the expression changes observed in this study. Farnesoic acid is then oxidized from the ω-carbon to produce a C_{15} dicarboxylic acid. We identified several CYP4A orthologs induced by SQ1, which we propose catalyzes the ω-hydroxylation of farnesoic acid followed by sequential oxidation at the ω-carbon, possibly by the same enzymes involved in farnesol oxidation. The C_{15}-DCA could then be activated by ACSL1 to its CoA derivative for transport into the peroxisome via the dicarboxylic acid transporter ABCD3 (van Roermund et al., 2014), and then undergo one or two rounds of β-oxidation, producing C_{10} and C_{12} DCAs as well as propionyl-CoA and acetyl-CoA. The chain-shortened DCAs could either be conjugated with carnitine and exported to the mitochondria for further

oxidation or processed by ACOT enzymes, producing free acids that are then eliminated from the cell. For brevity, not all of the enzyme names and/or cofactors are shown for each step. Blue colored boxes represent orthologous genes that were identified through microarrays to be differentially higher in SQ1-treated compared to untreated controls or to Prav-treated cells ($P \geq 1.5$-fold). * A number of enzymes involved in peroxisomal and mitochondrial β-oxidation were differentially higher in SQ1-treated compared to control or Prav-treated cells but were excluded for clarity (see **Fig. 3** and **4** and text).

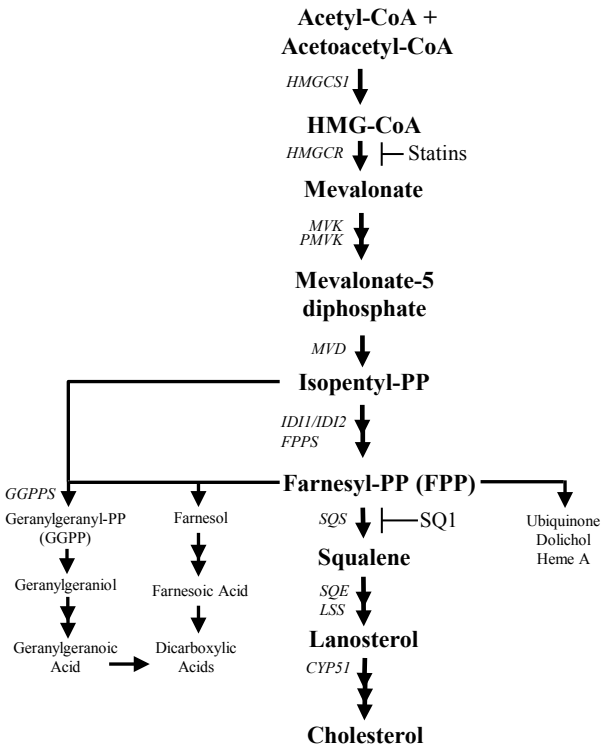
Acetyl-CoA +
Acetoacetyl-CoA
HMGCS1
HMG-CoA
HMGCR
Statins
Mevalonate
MVK
PMVK
Mevalonate-5
diphosphate
MVD
Isopentyl-PP
IDI1/IDI2
FPPS
Farnesyl-PP (FPP)
GGPPS
Geranylgeranyl-PP
(GGPP)
Geranylgeraniol
Geranylgeranoic
Acid
Farnesol
Farnesoic Acid
Dicarboxylic
Acids
SQS
SQ1
Squalene
SQE
LSS
Lanosterol
CYP51
Cholesterol
Ubiquinone
Dolichol
Heme A

Figure 1

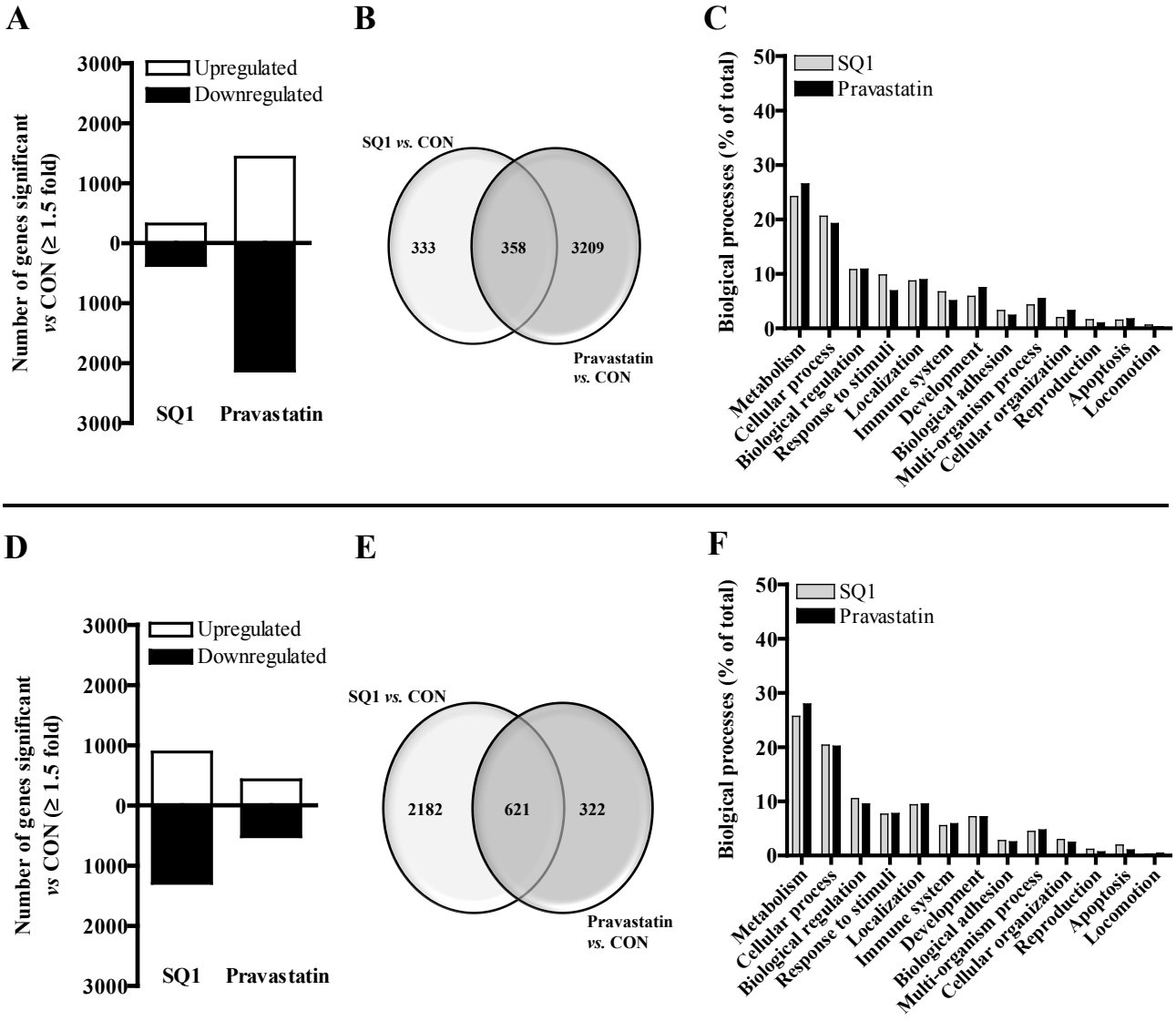
A
Number of genes significant vs CON (≥ 1.5 fold)
3000
2000
1000
0
1000
2000
3000
Upregulated
Downregulated
SQ1
Pravastatin
B
SQ1 vs. CON
333
358
3209
Pravastatin vs. CON
C
Biolgical processes (% of total)
50
40
30
20
10
0
SQ1
Pravastatin
Metabolism
Cellular process
Biological regulation
Response to stimuli
Localization
Immune system
Development
Biological adhesion
Multi-organism process
Cellular organization
Reproduction
Apoptosis
Locomotion
D
Number of genes significant vs CON (≥ 1.5 fold)
3000
2000
1000
0
1000
2000
3000
Upregulated
Downregulated
SQ1
Pravastatin
E
SQ1 vs. CON
2182
621
322
Pravastatin vs. CON
F
Biolgical processes (% of total)
50
40
30
20
10
0
SQ1
Pravastatin
Metabolism
Cellular process
Biological regulation
Response to stimuli
Localization
Immune system
Development
Biological adhesion
Multi-organism process
Cellular organization
Reproduction
Apoptosis
Locomotion

Figure 2

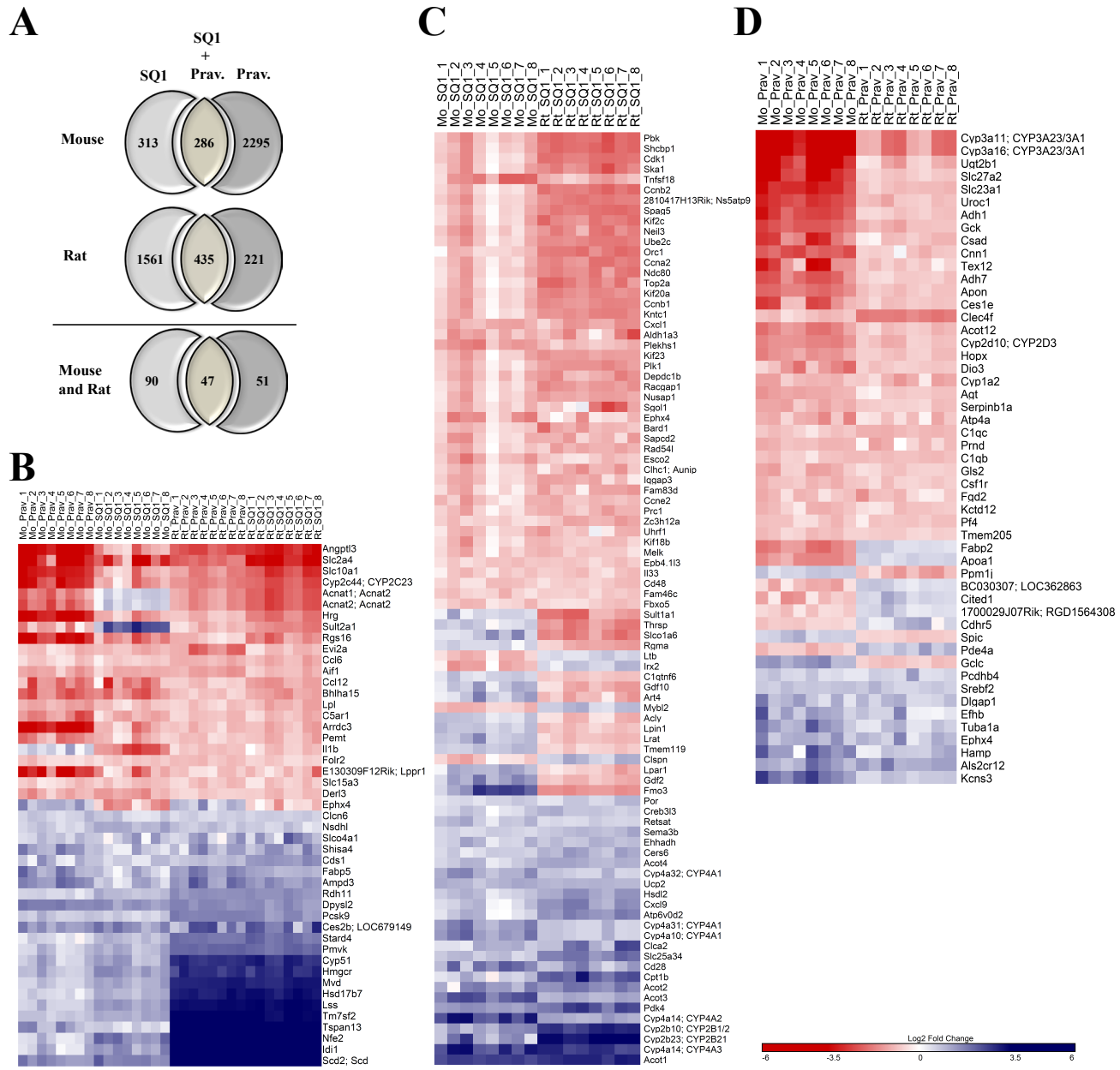
A
SQ1
+
SQ1
Prav.
Prav.
Mouse
313
286
2295
Rat
1561
435
221
Mouse
and Rat
90
47
51
B
Angptl3
Slc2a4
Slc10a1
Cyp2c44; CYP2C23
Acnat1; Acnat2
Acnat2; Acnat2
Hrg
Sult2a1
Rgs16
Evi2a
Ccl6
Aif1
Ccl12
Bhlha15
Lpl
C5ar1
Arrdc3
Pemt
Il1b
Folr2
E130309F12Rik; Lppr1
Slc15a3
Derl3
Ephx4
Clcn6
Nsdhl
Slco4a1
Shisa4
Cds1
Fabp5
Ampd3
Rdh11
Dpysl2
Pcsk9
Ces2b; LOC679149
Stard4
Pmvk
Cyp51
Hmgcr
Mvd
Hsd17b7
Lss
Tm7sf2
Tspan13
Nfe2
Idi1
Scd2; Scd
C
Pbk
Shcbp1
Cdk1
Ska1
Tnfsf18
Ccnb2
2810417H13Rik; Ns5atp9
Spag5
Kif2c
Neil3
Ube2c
Orc1
Ccna2
Ndc80
Top2a
Kif20a
Ccnb1
Kntc1
Cxcl1
Aldh1a3
Plekhs1
Kif23
Plk1
Depdc1b
Racgap1
Nusap1
Sgol1
Ephx4
Bard1
Sapcd2
Rad54l
Esco2
Clhc1; Aunip
Iqgap3
Fam83d
Ccne2
Prc1
Zc3h12a
Uhrf1
Kif18b
Melk
Epb4.1l3
Il33
Cd48
Fam46c
Fbxo5
Sult1a1
Thrsp
Slco1a6
Rgma
Ltb
Irx2
C1qtnf6
Gdf10
Art4
Mybl2
Acly
Lpin1
Lrat
Tmem119
Clspn
Lpar1
Gdf2
Fmo3
Por
Creb3l3
Retsat
Sema3b
Ehhadh
Cers6
Acot4
Cyp4a32; CYP4A1
Ucp2
Hsdl2
Cxcl9
Atp6v0d2
Cyp4a31; CYP4A1
Cyp4a10; CYP4A1
Clca2
Slc25a34
Cd28
Cpt1b
Acot2
Acot3
Pdk4
Cyp4a14; CYP4A2
Cyp2b10; CYP2B1/2
Cyp2b23; CYP2B21
Cyp4a14; CYP4A3
Acot1
D
Cyp3a11; CYP3A23/3A1
Cyp3a16; CYP3A23/3A1
Ugt2b1
Slc27a2
Slc23a1
Uroc1
Adh1
Gck
Csad
Cnn1
Tex12
Adh7
Apon
Ces1e
Clec4f
Acot12
Cyp2d10; CYP2D3
Hopx
Dio3
Cyp1a2
Aqt
Serpinb1a
Atp4a
C1qc
Prnd
C1qb
Gls2
Csf1r
Fqd2
Kctd12
Pf4
Tmem205
Fabp2
Apoa1
Ppm1j
BC030307; LOC362863
Cited1
1700029J07Rik; RGD1564308
Cdhr5
Spic
Pde4a
Gclc
Pcdhb4
Srebf2
Dlgap1
Efhb
Tuba1a
Ephx4
Hamp
Als2cr12
Kcns3
Log2 Fold Change
-6
-3.5
0
3.5
6

Figure 3

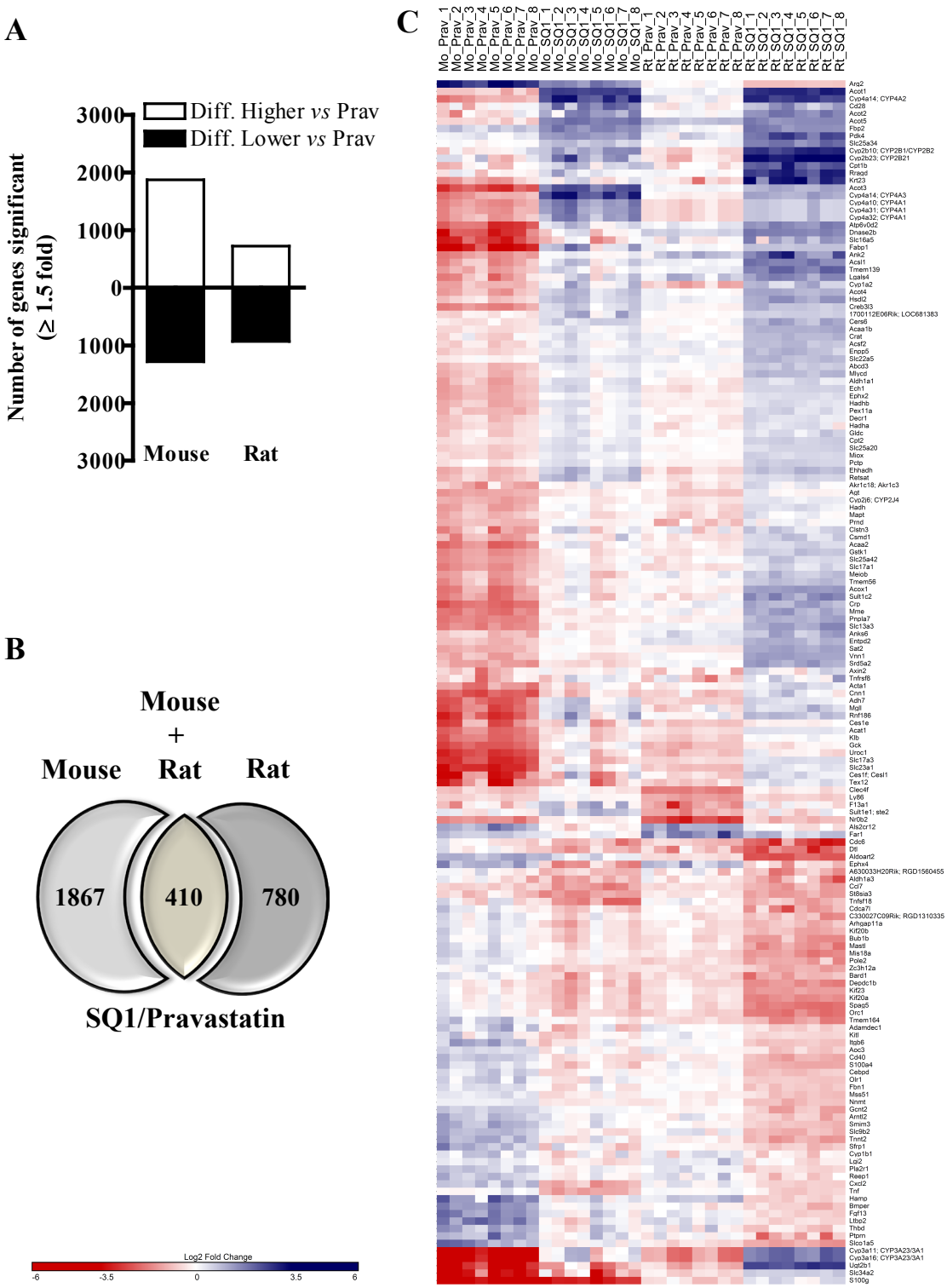
A
Diff. Higher vs Prav
Diff. Lower vs Prav
Number of genes significant (≥ 1.5 fold)
3000
2000
1000
0
1000
2000
3000
Mouse
Rat
B
Mouse
+
Mouse
Rat
Rat
1867
410
780
SQ1/Pravastatin
Log2 Fold Change
-6
-3.5
0
3.5
6
C
Mo_Prav_1
Mo_Prav_2
Mo_Prav_3
Mo_Prav_4
Mo_Prav_5
Mo_Prav_6
Mo_Prav_7
Mo_Prav_8
Mo_SQ1_1
Mo_SQ1_2
Mo_SQ1_3
Mo_SQ1_4
Mo_SQ1_5
Mo_SQ1_6
Mo_SQ1_7
Mo_SQ1_8
Rt_Prav_1
Rt_Prav_2
Rt_Prav_3
Rt_Prav_4
Rt_Prav_5
Rt_Prav_6
Rt_Prav_7
Rt_Prav_8
Rt_SQ1_1
Rt_SQ1_2
Rt_SQ1_3
Rt_SQ1_4
Rt_SQ1_5
Rt_SQ1_6
Rt_SQ1_7
Rt_SQ1_8

Figure 4

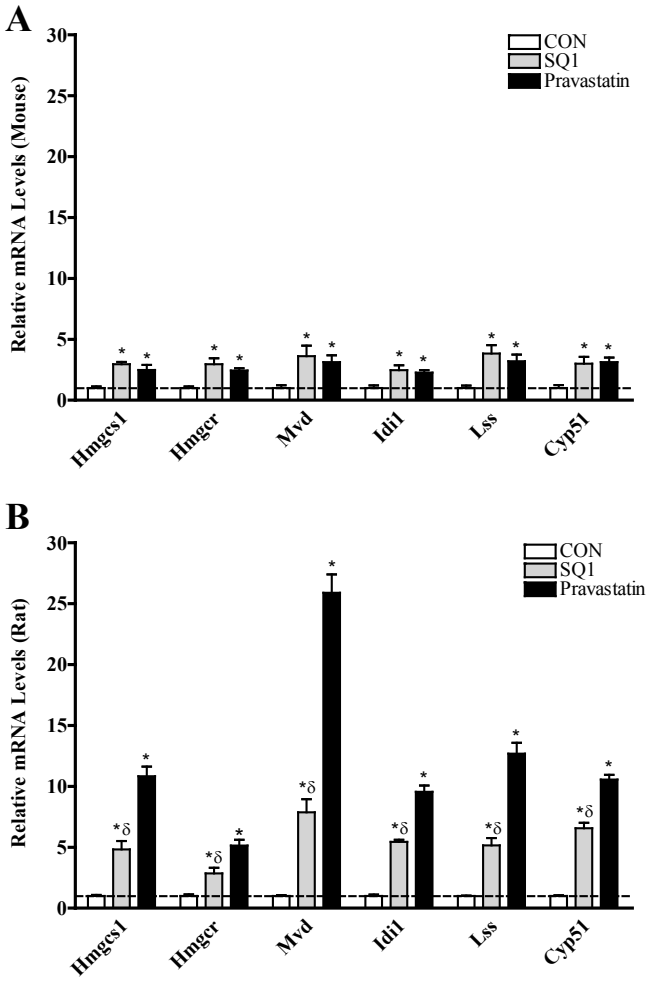
A
Relative mRNA Levels (Mouse)
CON
SQ1
Pravastatin
Hmgcs1
Hmgcr
Mvd
Idi1
Lss
Cyp51
B
Relative mRNA Levels (Rat)
CON
SQ1
Pravastatin
Hmgcs1
Hmgcr
Mvd
Idi1
Lss
Cyp51

Figure 5

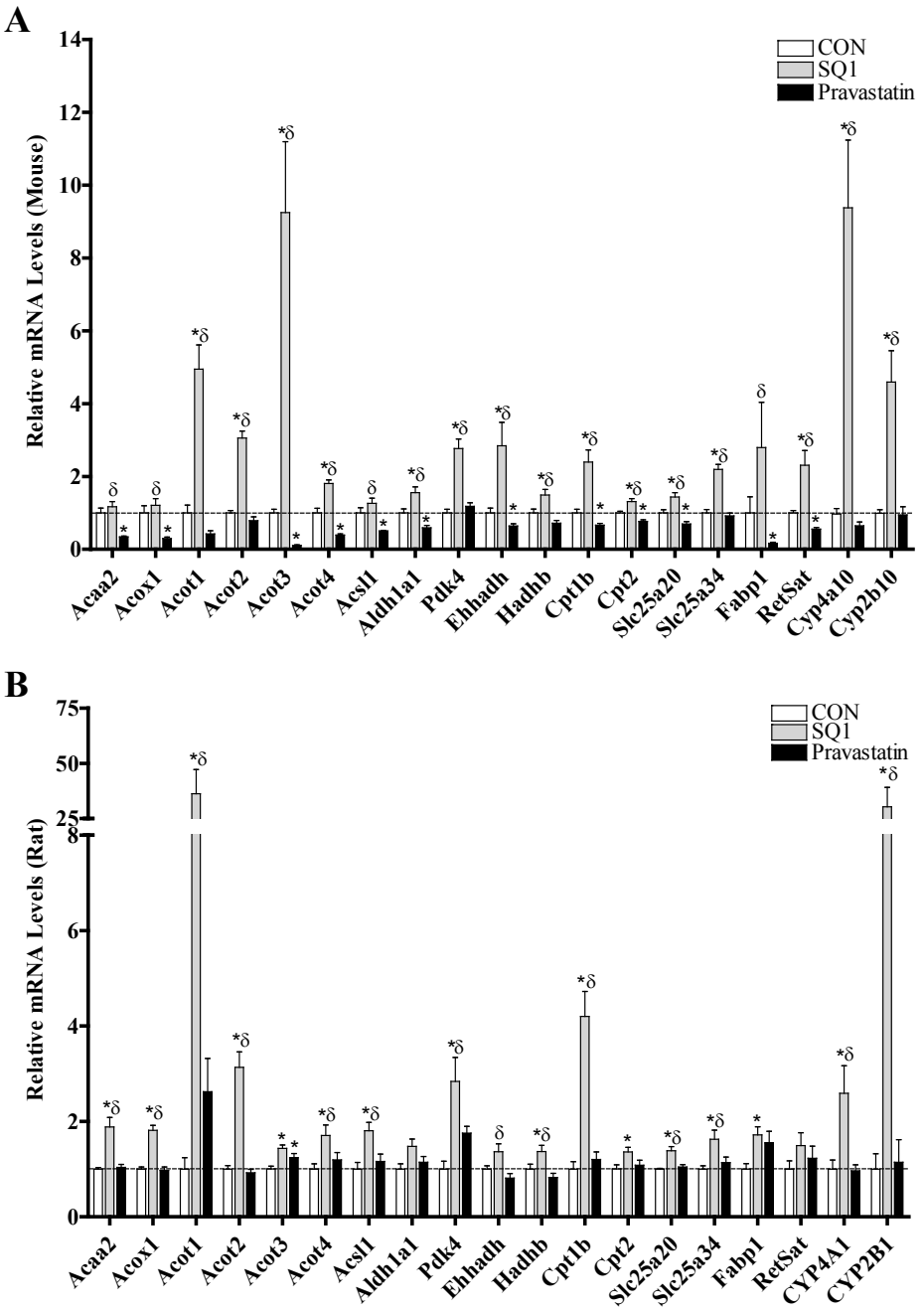
A
CON
SQ1
Pravastatin
Relative mRNA Levels (Mouse)
Acaa2
Acox1
Acot1
Acot2
Acot3
Acot4
Acsl1
Aldh1a1
Pdk4
Ehhadh
Hadhb
Cpt1b
Cpt2
Slc25a20
Slc25a34
Fabp1
RetSat
Cyp4a10
Cyp2b10
B
CON
SQ1
Pravastatin
Relative mRNA Levels (Rat)
Acaa2
Acox1
Acot1
Acot2
Acot3
Acot4
Acsl1
Aldh1a1
Pdk4
Ehhadh
Hadhb
Cpt1b
Cpt2
Slc25a20
Slc25a34
Fabp1
RetSat
CYP4A1
CYP2B1

Figure 6

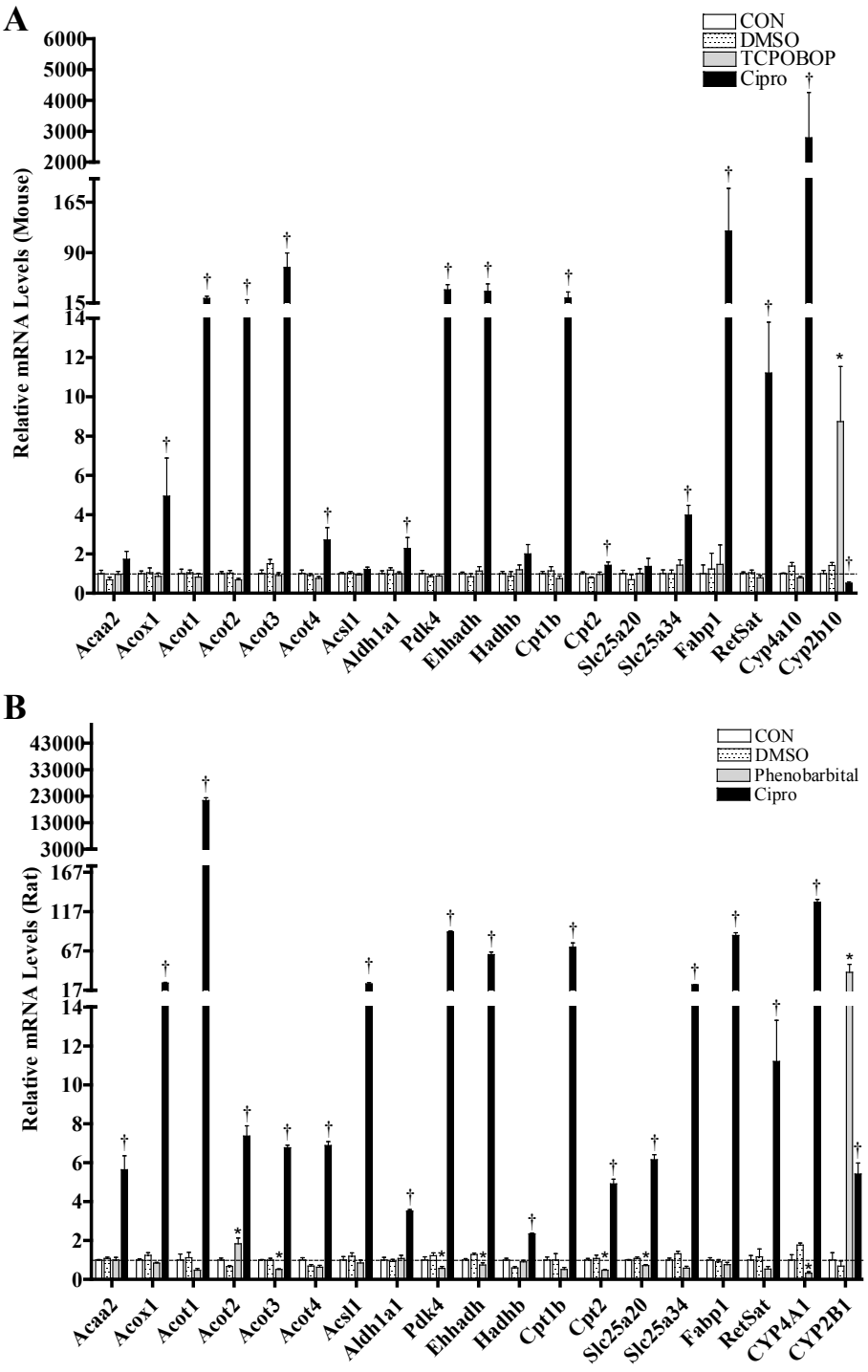
A
CON
DMSO
TCPOBOP
Cipro
Relative mRNA Levels (Mouse)
6000
5000
4000
3000
2000
165
90
15
14
12
10
8
6
4
2
0
Acaa2
Acox1
Acot1
Acot2
Acot3
Acot4
Acsl1
Aldh1a1
Pdk4
Ehhadh
Hadhb
Cpt1b
Cpt2
Slc25a20
Slc25a34
Fabp1
RetSat
Cyp4a10
Cyp2b10
B
CON
DMSO
Phenobarbital
Cipro
Relative mRNA Levels (Rat)
43000
33000
23000
13000
3000
167
117
67
17
14
12
10
8
6
4
2
0
Acaa2
Acox1
Acot1
Acot2
Acot3
Acot4
Acsl1
Aldh1a1
Pdk4
Ehhadh
Hadhb
Cpt1b
Cpt2
Slc25a20
Slc25a34
Fabp1
RetSat
CYP4A1
CYP2B1

Figure 7

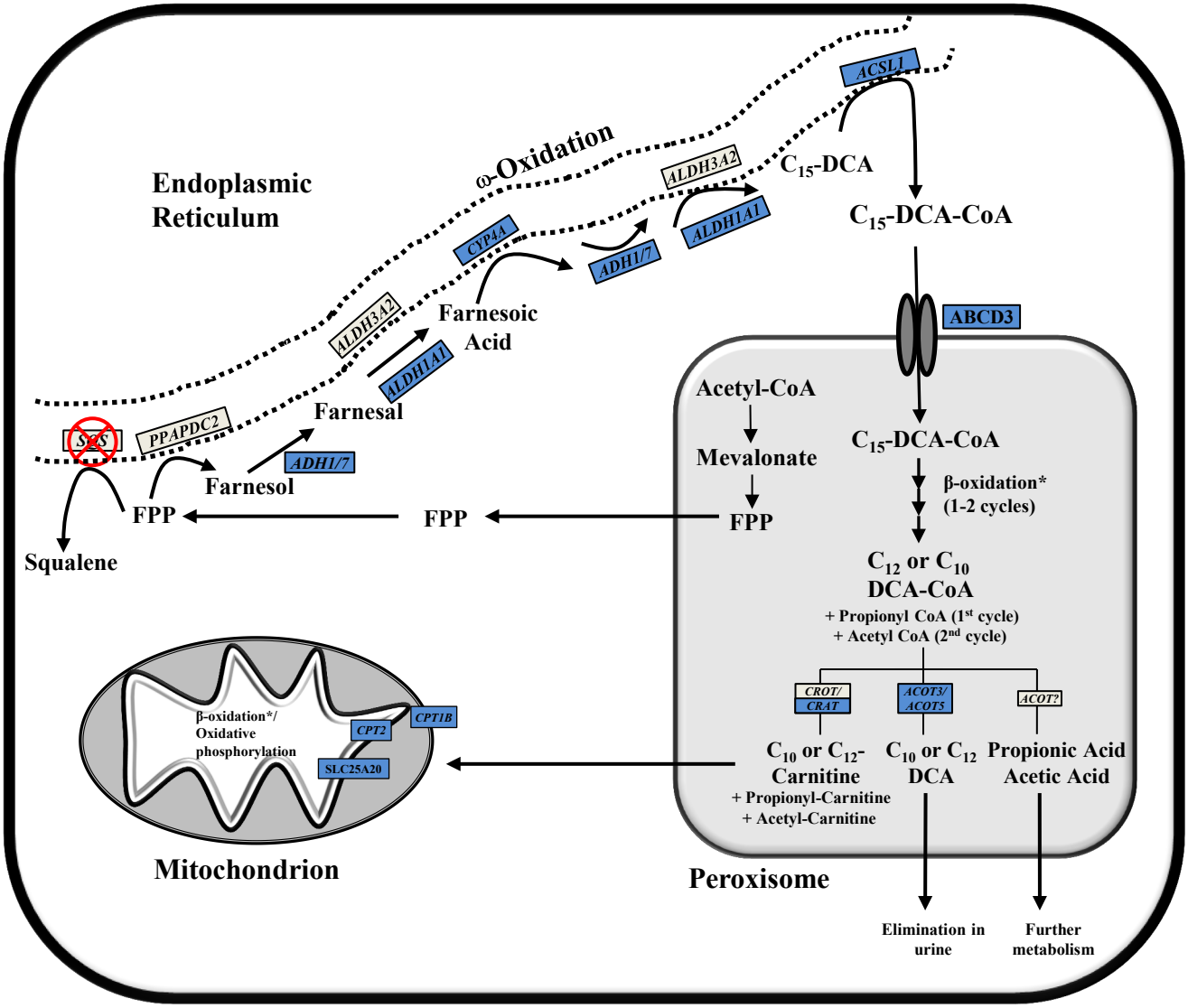
Endoplasmic Reticulum
ω-Oxidation
ACSL1
C15-DCA
C15-DCA-CoA
ALDH3A2
ALDH1A1
CYP4A
ADH1/7
Farnesoic Acid
ALDH3A2
ALDH1A1
Farnesal
SQS
PPAPDC2
ADH1/7
Farnesol
FPP
FPP
FPP
Squalene
ABCD3
Acetyl-CoA
Mevalonate
C15-DCA-CoA
β-oxidation*
(1-2 cycles)
C12 or C10
DCA-CoA
+ Propionyl CoA (1st cycle)
+ Acetyl CoA (2nd cycle)
CROT/
CRAT
ACOT3/
ACOT5
ACOT?
C10 or C12-
Carnitine
+ Propionyl-Carnitine
+ Acetyl-Carnitine
C10 or C12
DCA
Propionic Acid
Acetic Acid
β-oxidation*/
Oxidative
phosphorylation
CPT2
CPT1B
SLC25A20
Mitochondrion
Peroxisome
Elimination in urine
Further metabolism

Figure 8

Rondini EA, Duniec-Dmuchowski Z, Cukovic D, Dombkowski A, and Kocarek TA. Differential regulation of gene expression by cholesterol biosynthesis inhibitors that reduce (pravastatin) or enhance (squalestatin 1) nonsterol isoprenoid levels in primary cultured mouse and rat hepatocytes. *The Journal of Pharmacology and Experimental Therapeutics.*

Supplemental Table 1. Mouse genes and primer pairs used for *q*RT-PCR.

Gene Name	Gene Title	NCBI Reference Sequence	Forward Primer (5'→3')	Reverse Primer (5'→3')
Acaa2	acetyl-Coenzyme A acyltransferase 2	NM_177470	CCCTGCTACGAGGTGTGTTC	ACATTGCCCACGATGACACT
Acot1	acyl-CoA thioesterase 1	NM_012006	TTTGGAGGTTGGGGAAAGGT	CCAGCCCTTGAATCAGCACTA
Acot2	acyl-CoA thioesterase 2	NM_134188	AAGAAGCCGTGAACTACCTGC	TGACTTGGTTTCTCAGAAGGGACA
Acot3	acyl-CoA thioesterase 3	NM_134246	GCTCAGTCACCCTCAGGTAA	AAGTTTCCGCCGATGTTGGA
Acot4	acyl-CoA thioesterase 4	NM_134247	TCCAAAGGTAAAAGGCCCAG	GCGGAATCATGGTCTGCTTG
Acox1	acyl-Coenzyme A oxidase 1, palmitoyl	NM_001271898	GGAACCTGTTGGCCTCAATTAC	CTCGAAGATGAGTTCCGTGGC
Acsl1	acyl-CoA synthetase long-chain family member 1	NM_007981	GCCGCGACTCCTTAAATAGCA	ATGCAGAATTCTCCTCCGCTG
Aldh1a1	aldehyde dehydrogenase family 1, subfamily A1	NM_013467	TGACCAGGTGCTTTCCATTGTA	TGCAGTCATTATGTGTGGTGAGT
Cpt1b	carnitine palmitoyltransferase 1b, muscle	NM_009948	TGTCTACCTCCGAAGCAGGA	GCCATGACCGGCTTGATCT
Cpt2	carnitine palmitoyltransferase 2	NM_009949	TGACAGCCAGTTCAGGAAGAC	GGCCTGAGATGTAGCTGGTG
Cyp2b10	cytochrome P450, family 2, subfamily b, polypeptide 10	NM_009999	GCTTTGAGTACACAGACCGT	CTCAAACATCTGGCTGGAGA
Cyp4a10	cytochrome P450, family 4, subfamily a, polypeptide 10	NM_010011	CTTCCCAAGTGCCTTTCCTAGAT	GGCTGTCCATTCAACAAGAGC
Cyp51	cytochrome P450, family 51	NM_020010	GTTTCAGGCGCAGGGATAGA	CATCTGTTAGAGGACGCCCG
Ehhadh	enoyl-Coenzyme A, hydratase/3-hydroxyacyl Coenzyme A dehydrogenase	NM_023737	GGTCAATGCCATCAGTCCAAC	CTGGCTTCTGGTATCGCTGT

Rondini EA, Duniec-Dmuchowski Z, Cukovic D, Dombkowski A, and Kocarek TA. Differential regulation of gene expression by cholesterol biosynthesis inhibitors that reduce (pravastatin) or enhance (squalestatin 1) nonsterol isoprenoid levels in primary cultured mouse and rat hepatocytes. *The Journal of Pharmacology and Experimental Therapeutics.*

Supplemental Table 1. Mouse genes and primer pairs used for *q*RT-PCR (continued).

Gene Name	Gene Title	NCBI Reference Sequence	Forward Primer (5'→3')	Reverse Primer (5'→3')
Fabp1	fatty acid binding protein 1, liver	NM_017399	GTGGTCAGCTGTGGAAAGGA	GTCCTCGGGCAGACCTATTG
Hadhb	hydroxyacyl-Coenzyme A dehydrogenase/3-ketoacyl-Coenzyme A thiolase/enoyl-Coenzyme A hydratase (trifunctional protein), beta subunit	NM_145558	TTCGCGGACTCTAAGATTTCA	GCAGAGTGCAGTTGGGAAGA
Hmgcr	3-hydroxy-3-methylglutaryl-Coenzyme A reductase	NM_008255	ATCCTGACGATAACGCGGTG	AAGAGGCCAGCAATACCCAG
Hmgcs1	3-hydroxy-3-methylglutaryl-Coenzyme A synthase 1	NM_145942	TGATCCCCTTTGGTGGCTGA	AGGGCAACGATTCCCACATC
Idi1	isopentenyl-diphosphate delta isomerase	NM_145360	GACGTCAGGCTTGTGCTAGA	CTAGAACACAGAGATTCCGGCT
Lss	lanosterol synthase (2,3-oxidosqualene-lanosterol cyclase)	NM_146006	GGGCTGGTGATTATGGTGGT	CTCGATGTGCAAGCCCCA
Mvd	mevalonate (diphospho) decarboxylase	NM_138656	CTGCACCAGGACCAGCTAAA	CTGAGGCTGAGGGGTAGAGT
Pdk4	pyruvate dehydrogenase kinase, isoenzyme 4	NM_013743	TAGGTGGGCGTCAGGATGAA	TCTGAACCAAAGTCCAGCAG
Retsat	retinol saturase (all trans retinol 13,14 reductase)	NM_026159	GAATGGTTCGAGGAGTGGCA	CCAGTCACACTCTCCACCTTG
Slc25a20	solute carrier family 25 (mitochondrial carnitine/acylcarnitine translocase), member 20	NM_020520	CATGTGCCTGGTGTTTGTGG	CCCTGTGATGCCCTCTCTCA
Slc25a34	solute carrier family 25, member 34	NM_001013780	GGCCTCATGAATGGTGTCCG	AGCTGTGTCTTGACCAGGTA

Rondini EA, Duniec-Dmuchowski Z, Cukovic D, Dombkowski A, and Kocarek TA. Differential regulation of gene expression by cholesterol biosynthesis inhibitors that reduce (pravastatin) or enhance (squalestatin 1) nonsterol isoprenoid levels in primary cultured mouse and rat hepatocytes. *The Journal of Pharmacology and Experimental Therapeutics.*

Supplemental Table 2. Rat genes and primer pairs used for *q*RT-PCR.

Gene Name	Gene Title	NCBI Reference Sequence	Forward Primer (5'→3')	Reverse Primer (5'→3')
Acaa2	acetyl-CoA acyltransferase 2	NM_130433	GCTCCTCAGTTCTTGGCTGT	CCACCTCGACGCCTTAACTC
Acot1	acyl-CoA thioesterase 1	NM_031315	ACCCTGAGGTAAAAGGACCA	GGTTTCTCAGGATAGTCACAGGG
Acot2	acyl-CoA thioesterase 2	NM_138907	CCTGGTGGGTGCTAACATCA	AGGGGGCACCTCCTAACTC
Acot3	acyl-CoA thioesterase 3	NM_001108041	ACCCTCAGGTAAAAGGTTCAGG	TGATTCGTTTGGTGCTCATGC
Acot4	acyl-CoA thioesterase 4	NM_001109440	CCCGAAGGTAAAAGGCCCAG	CCTGAGAAAGCCACCTTCGT
Acox1	acyl-CoA oxidase 1, palmitoyl	NM_017340	CGCCGTCGAGAAATTGAGAAC	AGGCCAACAGGTTCCACAAA
Acsl1	acyl-CoA synthetase long-chain family member 1	NM_012820	AATGGCTGAGTGCATAGGCT	GATGGTCACCCACTCAGGTC
Aldh1a1	aldehyde dehydrogenase 1 family, member A1	NM_022407	GATGCCGACTTGGACATTGC	TGGCTCGCTCAACACTCTTT
Cpt1b	carnitine palmitoyltransferase 1b, muscle	NM_013200	ACGGATACGGGGTTTCCTAC	GCAGGGCGTTCGTTTCT
Cpt2	carnitine palmitoyltransferase 2	NM_012930	ACAGCCAGTTCAGGAGAACA	GGCCTGAGATGTAGCTGGTG
CYP2B1	cytochrome P450, family 2, subfamily b, polypeptide 1	NM_001134844.1	CAACCCTTGATGACCGCAGTA	TTCAGTGTTCTTGGGAAGCAG
CYP4A1	cytochrome P450, family 4, subfamily a, polypeptide 1	NM_175837	CGCTTTGAGCTACTGCCAGA	TCGGAGCTCCACAACGGAAT
Cyp51	cytochrome P450, family 51	NM_012941	GATGGAGCAGGTGACAGGAG	ATATGGCGGACTTTTCGCTC
Ehhadh	enoyl-CoA, hydratase/3-hydroxyacyl CoA dehydrogenase	NM_133606	CCCTGGCCTTGCATTAGGAA	CGACACGAGCCTTTGCATTG

Rondini EA, Duniec-Dmuchowski Z, Cukovic D, Dombkowski A, and Kocarek TA. Differential regulation of gene expression by cholesterol biosynthesis inhibitors that reduce (pravastatin) or enhance (squalestatin 1) nonsterol isoprenoid levels in primary cultured mouse and rat hepatocytes. *The Journal of Pharmacology and Experimental Therapeutics.*

Supplemental Table 2. Rat genes and primer pairs used for *q*RT-PCR (continued).

Gene Name	Gene Title	NCBI Reference Sequence	Forward Primer (5'→3')	Reverse Primer (5'→3')
Fabp1	fatty acid binding protein 1, liver	NM_012556	TTCATGAAGGCGATGGGTCT	GTCTCCAGTTCGCACTCCTC
Hadhb	hydroxyacyl-CoA dehydrogenase/3-ketoacyl-CoA thiolase/enoyl-CoA hydratase (trifunctional protein), beta subunit	NM_133618	TATCTGGGGCGGATCACTCT	CATAGCATGACCCTGTCCTCC
Hmgcr	3-hydroxy-3-methylglutaryl-CoA reductase	NM_013134	AGTGCAGAGAAAGGTGCGAA	TGCGTCTCCATGAGGGTTTC
Hmgcs1	3-hydroxy-3-methylglutaryl-CoA synthase 1	NM_017268	TCGCGTTTGGTGCCTGAA	AGGGCAACGATTCCCACATC
Idi1	isopentenyl-diphosphate delta isomerase 1	NM_053539	GTGACGTCAGGACTACGCTA	TCTGACCTAGAACACAGCGAT
Lss	lanosterol synthase (2,3-oxidosqualene-lanosterol cyclase)	NM_031049	CTGGCCTCAGGAGAACATCT	CTCAAATGTGGCCAGCAAGG
Mvd	mevalonate (diphospho) decarboxylase	NM_031062	CCAAGAGCAGGACTTCCAGG	AATGTGTACGCCACCTTCGT
Pdk4	pyruvate dehydrogenase kinase, isozyme 4	NM_053551	GCAGTCCTCACCAACCCTAC	TCTGAACCGAAGTCCAGCAG
Retsat	retinol saturase (all trans retinol 13,14 reductase)	NM_145084	CGATTCCCAGACCGATCCAC	CACCGACATAGAGGCTTCCC
Slc25a20	solute carrier family 25 (carnitine/acylcarnitine translocase), member 20	NM_053965	GGGCAGCCACCTATGTACTC	AGCTGCGGGTAGGTAAGTTC
Slc25a34	solute carrier family 25, member 34	NM_001013936	GATCAACAGTGGTTTCTGGAGGA	GCTGACGACATCGAAGGGAG